Journal of Structural Geology 32 (2010) 490–506

Contents lists available at ScienceDirect

Journal of Structural Geology

journal homepage: www.elsevier.com/locate/jsg

Normal fault growth and fault-related folding in a salt-influenced rift basin: South Viking Graben, offshore Norway

Karla E. Kane [a,*], Christopher A-L. Jackson [a], Eirik Larsen [b,1]

[a] Department of Earth Science & Engineering, Imperial College, London SW7 2AZ, UK
[b] Statoil ASA, Forusbeen 50, N-4035 Stavanger, Norway

ARTICLE INFO

Article history:
Received 7 February 2009
Received in revised form
19 February 2010
Accepted 22 February 2010
Available online 1 March 2010

Keywords:
Syn-rift
North Sea
Normal faulting
Fault-propagation folding
Salt tectonics

ABSTRACT

Three-dimensional seismic data were analysed to reconstruct the structural and stratigraphical development of a salt-influenced rift basin and thus gain an understanding of the relationships between normal fault growth, salt tectonics and the evolution of syn-rift depocentres. The Sleipner Basin, South Viking Graben, northern North Sea, is *ca.* 30 km long by 8 km wide and is bound to the east by a major extensional fault zone (Sleipner Fault Zone). Two types of fault-related fold are identified within the basin: (1) A fault-parallel monocline, interpreted as an extensional forced-fold, which formed through the upward propagation of the Sleipner Fault Zone through ductile evaporites of the Zechstein Supergroup and (2) three fault-perpendicular, salt-cored anticlines that compartmentalise the basin into four sub-basins and are related to displacement gradients along-strike of the Sleipner Fault Zone. Detailed seismic-stratigraphic analysis of pre- and syn-rift stratal units reveals a complex interplay between fault growth and salt movement which strongly controlled the evolution of syn-rift depocentres. During the early syn-rift, a series of depocentres, separated along-strike by the fault-perpendicular folds, were offset into the axis of the basin (*ca.* 3–4.5 km to the west of the Sleipner Fault Zone) by the fault-propagation fold. Later in the rift event, the influence of the fault-perpendicular folds depleted, resulting in a larger, interconnected depocentre that shifted into the immediate hangingwall of the fault as the surface of the fault-propagation fold was breached. The results of this study have implications for normal fault growth and sedimentary depocentre development in salt-influenced rift basins, and contribute to the general understanding of the controls on salt migration.

1. Introduction

1.1. Fault-related folding in extensional basins

Large (i.e. several tens of kilometres length) basin-bounding fault zones in extensional basins typically develop through the interaction and linkage of a series of initially isolated normal fault segments (e.g. Peacock and Sanderson, 1991; Anders and Schlische, 1994; Cartwright et al., 1995; Dawers and Anders, 1995). This fault growth process commonly results in the development of intra-basin hangingwall folds with axes that are oriented broadly perpendicular to the strike of the basin-bounding fault (e.g. Gawthorpe and Hurst, 1993; Anders and Schlische, 1994; Gawthorpe et al., 1994; Schlische, 1995); 'transverse anticlines' or 'intra-basin highs' develop adjacent to segment boundaries or areas of displacement minima, whereas 'transverse synclines' or 'intra-basin lows' are associated with displacement maxima located at the centre of the constituent fault segments (e.g. Anders and Schlische, 1994; Gawthorpe et al., 1994; Schlische, 1995). In addition, fault-parallel folds, with axes that are oriented broadly parallel to the strike of the basin-bounding fault, are often observed. These structures typically form breached or unbreached basinward-facing monoclines which develop as a result of folding ahead of the upward propagating fault tip (e.g. Withjack et al., 1990; Schlische, 1995; Gawthorpe et al., 1997; Corfield and Sharp, 2000). Previous studies have shown that the development of these fault-propagation or forced folds (*sensu* Withjack et al., 1990; Withjack and Callaway, 2000) can significantly influence the distribution and thickness of sediment within the evolving basin, particularly during the early phase of rifting (e.g. Withjack et al., 1990; Gupta et al., 1999; Sharp et al., 2000; Dawers and Underhill, 2000; Ford et al., 2007).

* Corresponding author. Present address: Statoil (U.K.) Ltd, 1 Kingdom Street, W2 6BD London, UK. Tel.: +44 (0) 203 204 3531.
E-mail address: karkan@statoil.com (K.E. Kane).
[1] Present address: Rocksource ASA, Olav Kyrresgate 22, N-5808 Bergen, Norway.

0191-8141/$ – see front matter © 2010 Elsevier Ltd. All rights reserved.
doi:10.1016/j.jsg.2010.02.005

1.2. Salt mobility and fault-related folding

Models of normal fault growth and fault-related folding have largely been developed for rift basins involving extension of brittle, 'basement-type' lithologies. However, several studies have indicated that the structural style of a rift basin can be significantly influenced by the presence of ductile components such as evaporites (herein referred to as 'salt') within the pre-rift sedimentary succession (e.g. Koyi et al., 1993; Withjack and Callaway, 2000; Stewart et al., 1996, 1997; Richardson et al., 2005; Marsh et al., 2009). The viscous nature of such a substrate can restrict the upward propagation of a fault tip, resulting in a sub-salt, basement-involved fault that is decoupled from a forced-fold within the supra-salt cover strata (Withjack et al., 1990; Withjack and Callaway 2000; Stewart et al., 1996, 1997; Ford et al., 2007). Through time, the basement fault often propagates through the mechanically weak layer, leading to breaching of the earlier formed fold and the generation of a fault scarp at-surface (Jackson and Vendeville, 1994; Stewart et al., 1996, 1997; Pascoe et al., 1999). The development of normal faults and forced-folds commonly leads to salt migration which accommodates spatial variations in strain. Experimental modelling and seismic analysis have indicated that the geometry and distribution of normal faults and associated forced folds are dependent on several variables, including magnitude and rate of fault displacement; thickness contrast between the ductile layer and the brittle cover strata; physical properties of the ductile substrate (e.g. density and viscosity); and degree of differential loading in the overburden (Vendeville et al., 1995; Koyi et al., 1993; Stewart et al., 1996; Richardson et al., 2005; Withjack and Callaway, 2000).

1.3. Study aims

Many studies have provided what is essentially a two-dimensional understanding of the relationship between extensional faulting and salt mobility (e.g. Vendeville and Jackson, 1992a,b; Pascoe et al., 1999; Withjack and Callaway, 2000). However, given the along-strike complexity associated with the evolution of major normal fault systems, it should be expected that a significant component of salt movement will occur out of section during rifting. Here, 3D seismic and well data are used to investigate the relationships between normal fault growth and evaporite mobility within the Sleipner Basin, a sub-basin of the South Viking Graben, offshore Norway (Fig. 1). This area is particularly complex because late Middle to Late Jurassic rifting was initiated across a pre-existing structural template related to earlier, Triassic to Middle Jurassic salt movement. Critical to this study is the recognition that fault growth and salt migration results in variable rates and magnitude of subsidence that is documented by the coeval syn-rift succession. Changes in the thickness and seismic-stratigraphic architecture of the syn-rift units are used to constrain the temporal and spatial variation of surface deformation associated with the developing structures (see Gupta et al., 1998; Dawers and Underhill, 2000; Sharp et al., 2000; McLeod et al., 2000, 2002; Young et al., 2002). The results of this study indicate that the development of fault-related folds in salt-influenced rift basins is intimately

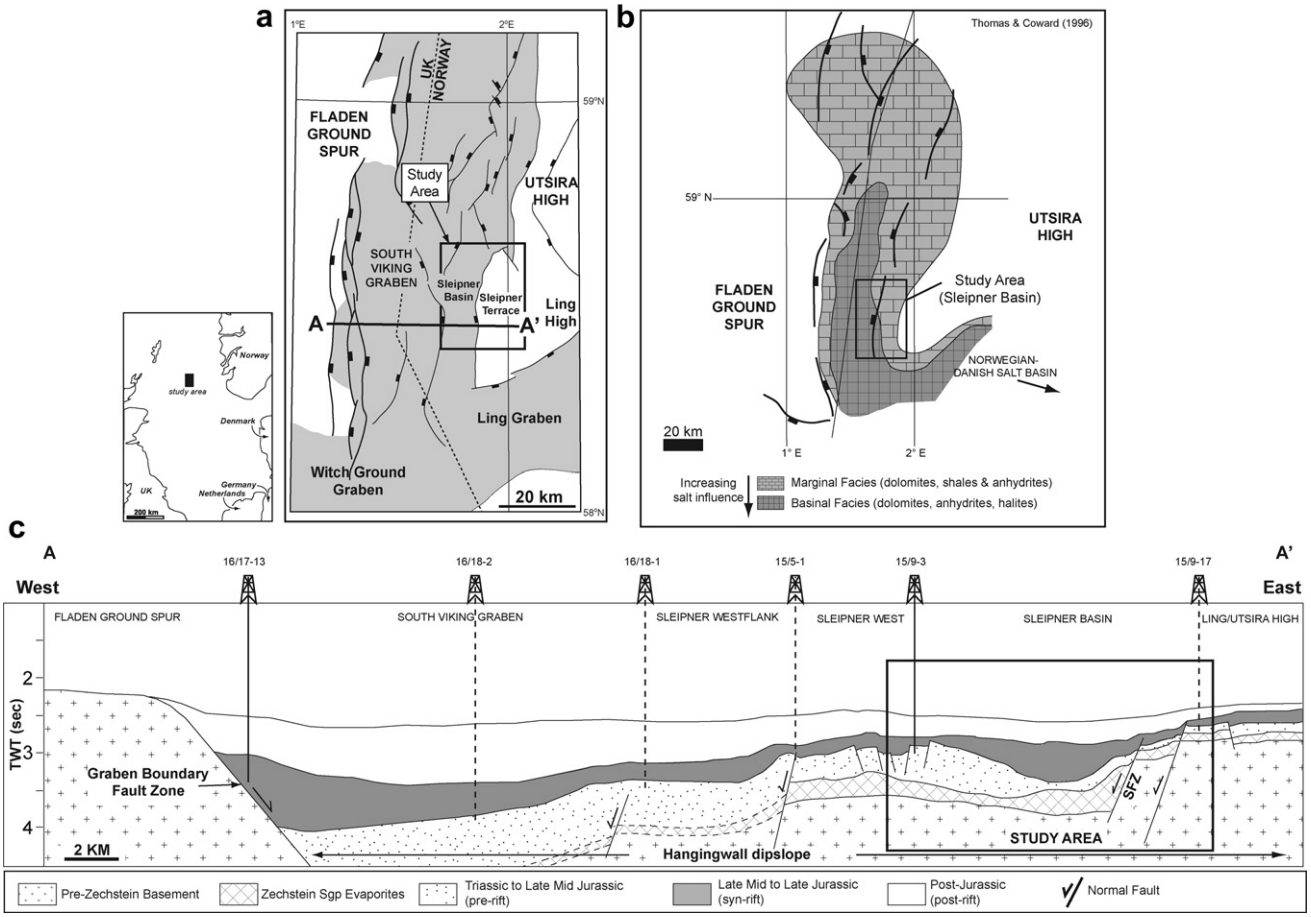

Fig. 1. Geological Setting of the Sleipner Basin (a) Map of South Viking Graben, northern North Sea (b) Map of Zechstein Supergroup facies distribution (redrawn from Thomas and Coward, 1996) (c) Regional cross-section showing location of Sleipner Basin study area on hangingwall dipslope of the South Viking Graben.

associated with the segmentation and linkage history of the extensional faults and that the spatial and temporal distribution of syn-rift sedimentary depocentres is largely controlled by the interplay between fault displacement and salt migration. In addition, it is apparent that sediment loading within syn-rift sedimentary depocentres may influence salt migration, particularly in the early phase of rift basin evolution.

2. Structural and stratigraphic setting

2.1. Permian-Triassic

The South Viking Graben initially formed in the Late Permian to Early Triassic as a NE-striking, fault-bounded embayment along the northern margin of the Northern Permian Salt Basin (Fig. 1; e.g. Pegrum and Ljones, 1984; Ziegler, 1990; Glennie, 1990, 1995; Hodgson et al., 1992; Roberts et al., 1995; Coward, 1995). The Sleipner Basin study area was located close to the axial part of the South Viking Graben where seismic and well data indicate that thick and mobile evaporite facies of the Zechstein Supergroup were deposited (Pegrum and Ljones, 1984; Thomas and Coward, 1996). Exploration wellbore 15/5–3, located approx. 5 km NW of the Sleipner Basin, penetrated a 1050 m Zechstein Supergroup succession which consisted principally of halite with some anhydrite. Outside of the study area, these salt-rich facies pass into carbonate and anhydrite-dominated, 'marginal' evaporite facies (Figs. 1 and 2; e.g. Glennie, 1990; Ziegler, 1990; Hodgson et al., 1992; Jackson et al., in press). For example, exploration wellbore, 16/7-2, located 10 km SE of the study area, encountered approx. 100 m of interbedded anhydrite, dolomite, shales and limestones.

Minor westwards thickening of Upper Triassic units towards the western basin-bounding fault (herein termed the Graben Boundary Fault Zone; *sensu* Cherry, 1993; Fig. 1) suggests extension during its deposition, although the magnitude is deemed minor compared to the earlier Permian and later Jurassic rift events (e.g. Badley et al., 1988; Glennie, 1995; Thomas and Coward, 1996). Deposition occurred in a marginal lacustrine environment (Smith Bank Formation), before fluvial-alluvial conditions (Skagerrak Formation) were established in the Late Triassic (Fig. 2; e.g. Fisher and Mudge, 1998). Previous studies have indicated mobility of the Zechstein Supergroup

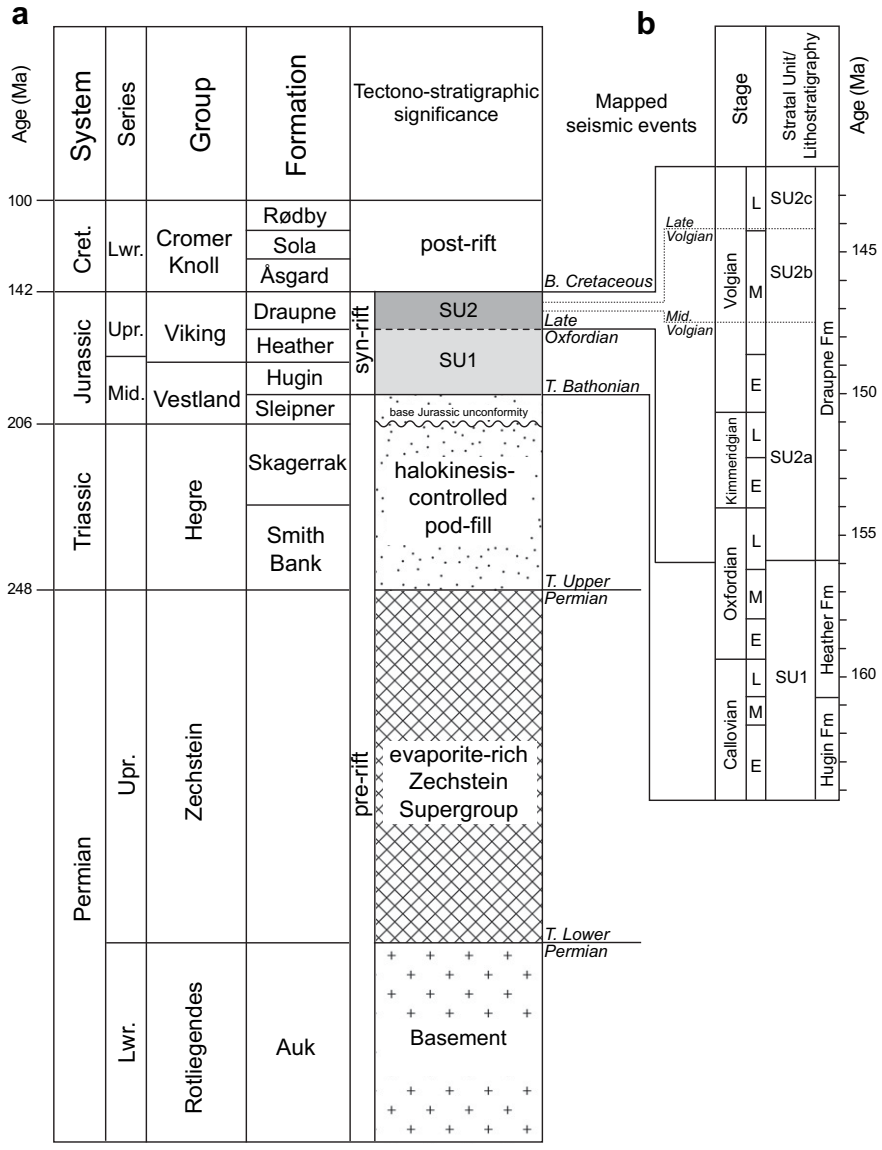

Fig. 2. Stratigraphic column and key seismic horizons. Pre-rift, syn-rift and post-rift intervals refer to the Late Jurassic rift episode. See text for full discussion. Note that short-duration, areally-restricted, intra-formational unconformities may be developed within the syn-rift stratigraphy due to fault-related folding (cf. progressive unconformities of Riba, 1976).

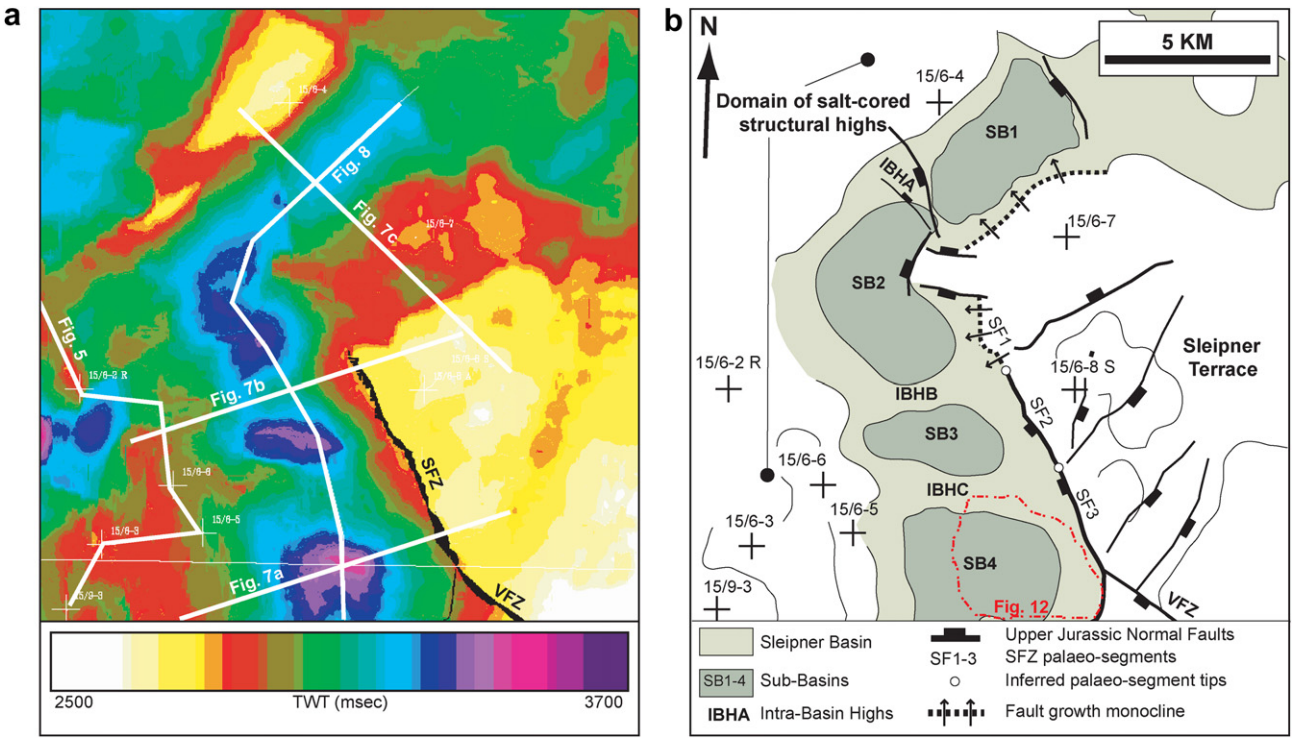

Fig. 3. (a) Time-structure map of the Top Bathonian horizon showing locations of seismic lines presented in Figs. 5, 7 and 8. (b) geological interpretation of (a), illustrating the main structural elements of the Sleipner Basin. The central and southern parts of the basin are bound to the east by the NNW-SSE trending Sleipner Fault Zone (comprised of three segments; labelled SF1-3) whilst the northern part of the basin is bound by a NE-SW trending monocline. A series of salt-cored highs form the western basin margin. Internally, the basin is divided into four sub-basins (labelled SB1-4) by a series of salt-cored intra-basin highs (i.e. IBHA-C). A fault-parallel fold is developed within the hangingwall of the Sleipner Fault Zone (SFZ). The location of Fig. 12 and the exploration wells used to calibrate mapped seismic reflection events are shown.

evaporites at this time, resulting in the formation of low-relief salt pillows, large salt diapirs and adjacent depocentres (Pegrum and Ljones, 1984; Thomas and Coward, 1996; Frostick et al., 1992; Fisher and Mudge, 1998; Jackson et al., in press). The control of Zechstein Supergroup mobility on Late Triassic depositional patterns has also been demonstrated in the Central North Sea (e.g. West Central Shelf; Stewart and Clark, 1999; Central Graben; Smith et al., 1993; Hodgson et al., 1992; Stewart and Clark, 1999; and the Forties-Montrose and Jaeren Highs; Stewart and Clark, 1999; Penge et al., 1999).

2.2. Early Jurassic–Late Jurassic

During the Early Jurassic, impingement of a mantle plume at the base of the lithosphere led to the formation of the Mid-North Sea Dome (e.g. Ziegler, 1990; Underhill and Partington, 1993), with subsequent uplift of the South Viking Graben and the development of an unconformity at the base of the Jurassic succession. During the early Middle Jurassic, a large delta, fed by sediment derived from the Mid-North Sea Dome, prograded northwards through the South Viking Graben and into the North Viking Graben. The fluvial systems that sourced the delta are partly preserved in the South Viking Graben as the Sleipner Formation (e.g. Helland-Hansen et al., 1992; Mitchener et al., 1992; Husmo et al., 2003).

During the late Middle Jurassic (Bajocian-Bathonian), marine transgression associated with collapse of the Mid-North Sea Dome and the reactivation of the Graben Boundary Fault Zone (Thomas and Coward, 1996) led to deposition of the shallow-marine Hugin Formation (Harris and Fowler, 1987; Cockings et al., 1992; Husmo et al., 2003) (Fig. 2). The initiation of rift-related normal faults influenced thickness and facies variations within these early syn-rift deposits (Harris and Fowler, 1987; Cockings et al., 1992; Thomas and Coward, 1996). During the latest Jurassic, an increase in fault-driven subsidence rates combined with a eustatic rise in sea-level, led to further deepening of the South Viking Graben and a progressive reduction in sedimentation rates. As a result, the Upper Jurassic is characterised by shelfal deposits of the Heather Formation, overlain by deep-marine mudstones of the Draupne

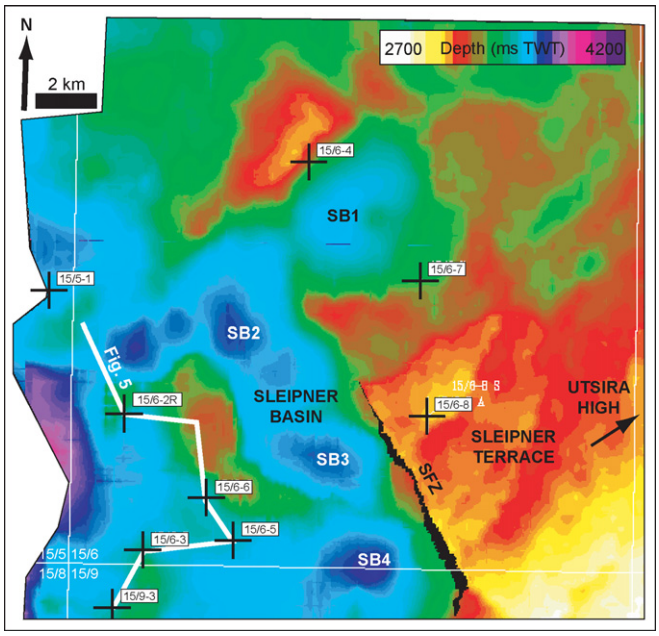

Fig. 4. Time structure map of the *top Upper Permian* (i.e. top Zechstein Supergroup evaporites) seismic horizon illustrating geometry and distribution of salt structures within the study area. The four sub-basins of the Sleipner Basin are labelled (SB1-4).

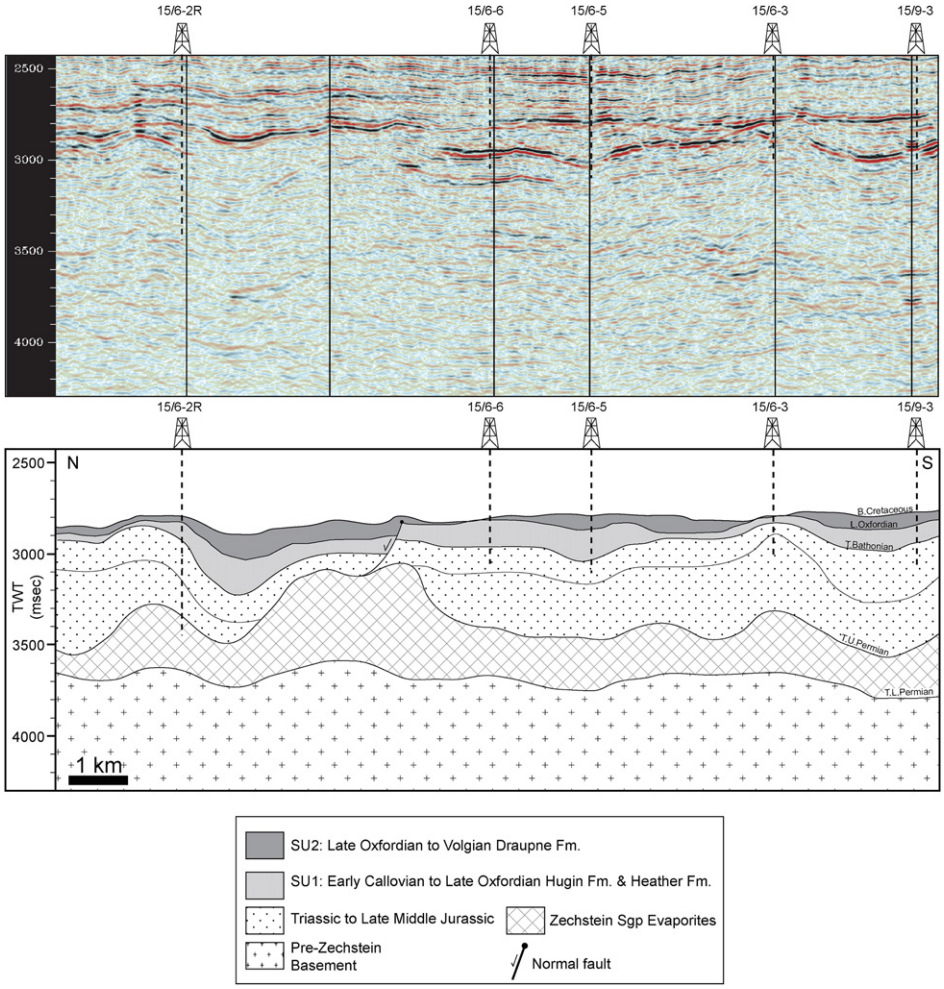

Fig. 5. Seismic profile across western basin-bounding high illustrating geometry of Zechstein Supergroup (Sgp) salt structures. Salt diapirism occurred mainly during the Triassic and Middle Jurassic as shown by the accumulation of thick sediment in the areas of salt withdrawal (pods) and progressive thinning towards the highs. For line location see Figs. 3, 4 and 6.

Formation (Fig. 2). The top of the syn-rift succession is marked by the Base Cretaceous Unconformity (BCU), which is conformable in this relatively basinal location.

During the latest Jurassic (early Middle Volgian; Jackson and Larsen, 2008), the majority of rift-related faults became inactive and the South Viking Graben experienced a period of compression (e.g. Pegrum and Ljones, 1984; Cherry, 1993; Knott et al., 1993, 1995; Thomas and Coward, 1996; Knott, 2001; Branther, 2003; Brehm, 2003; Fraser et al., 2003; Fletcher, 2003a,b; Jackson and Larsen, 2008). Although its origin remains unclear, this event was associated with large-wavelength folding and reverse and possibly strike-slip faulting (Pegrum and Ljones, 1984; Bartholomew et al., 1993; Cherry, 1993; Knott et al., 1993; Thomas and Coward, 1995, 1996; Knott et al., 1995; Knott, 2001; Branther, 2003; Fletcher, 2003a; Jackson and Larsen, 2008). The analysis presented below will demonstrate that the folds identified within the Sleipner Basin differ from those associated with this compressional event, in terms of both their timing and their mechanism of development, i.e. that they are late Middle to Late Jurassic in age and are extensional in origin.

3. Dataset and methodology

This study utilised a 450 km^2 3D seismic survey with a line spacing of 12.5 m, record length of 5.5 seconds, and a vertical resolution of *ca.* 35 m within the interval of interest (i.e. 2.5 to 4 seconds two-way travel-time (TWTT)). All seismic sections are displayed with reverse polarity (SEG European Convention; Brown, 2003), such that a downward increase in acoustic impedance is represented by a trough reflection event (black). Although the vertical scales of all seismic sections and maps are in TWTT, key observations such as fault offsets and sediment thicknesses have been estimated in metres based on velocity data derived from wells within the study area.

Stratigraphic ages of seven mapped seismic horizons (Fig. 2) were estimated using eleven wells distributed across the eastern and western margins of the Sleipner Basin (Fig. 3). The *top Lower Permian* and *top Upper Permian* horizons delimit the salt-rich Zechstein Supergroup, whilst the *top Bathonian* (near top Sleipner Formation) and *Base Cretaceous Unconformity* horizons bound the Upper Jurassic, syn-rift interval. Within the syn-rift, the *Late Oxfordian* (near top Heather Formation) seismic horizon forms a regionally mappable, intra-syn-rift reflection, sub-dividing the succession into two stratal units; *SU1* (i.e. early syn-rift, Early-Callovian to Late Oxfordian, Hugin and Heather formations) and *SU2* (i.e. late syn-rift, Late Oxfordian to Volgian, Draupne Formation). In addition, two late syn-rift, intra-*SU2* horizons (*Middle Volgian* and *Late Volgian*) were mapped locally in the south of the study area to subdivide *SU2* into three units (SU2a, b and c). Due to a lack of well data in this location, the stratigraphic ages of these intra-*SU2* horizons are tentative.

4. Triassic–early Middle Jurassic (pre-rift) structural style and evolution

As multiple phases of deformation occurred within the South Viking Graben during the Mesozoic, it is important to understand the geometry of the study area prior to the initiation of late Middle to Late Jurassic rifting. In particular, structures that developed in response to pre-rift salt migration during the Permian to early Middle Jurassic must be discriminated from structures related to the late Middle to Late Jurassic rift episode. This is achieved by determining the distribution and geometry of the salt-rich Zechstein Supergroup, and by analysing thickness patterns and seismic-stratigraphic architecture of the overlying Triassic to early Middle Jurassic (pre-rift) succession. Note that the terms 'pre-rift' and 'syn-rift' are used here with respect to the principal late Middle to Late Jurassic rift event, rather than the earlier Permo-Triassic rift event. Hence Permo-Triassic strata, although regionally deposited during an earlier rift event, are herein referred to collectively as 'pre-rift', and Cretaceous and younger units are referred to as 'post-rift'.

4.1. Regional distribution and geometry of the Zechstein Supergroup

Whilst an E–W oriented regional geoseismic section illustrates the overall dip of the salt-rich Zechstein Supergroup westwards towards the Graben Boundary Fault Zone (Fig. 1), a series of salt highs and low-relief salt pillows have been identified within the study area. These salt bodies are up to 2 km wide, 400 ms (540 m) high, 15 km^2 in plan-view and are distributed on the order of several kilometres (Figs. 4 and 5). Importantly, most are amorphous and even those that are slightly elongate appear to display no distinct or consistent trends, i.e. their geometry and distribution appears to be largely independent of the late Middle to Late Jurassic structural framework (Figs. 4 and 6). A notable exception to this occurs within the Sleipner Basin which is underlain by a relatively thin salt succession that thickens toward the immediate hanging-wall of the Sleipner Fault Zone (Fig. 7). In addition, a series of structural highs, cored by Zechstein Supergroup salt, are observed within the axis of the basin (Figs. 4 and 8). The geometry and origin of these structures will be described and discussed further below.

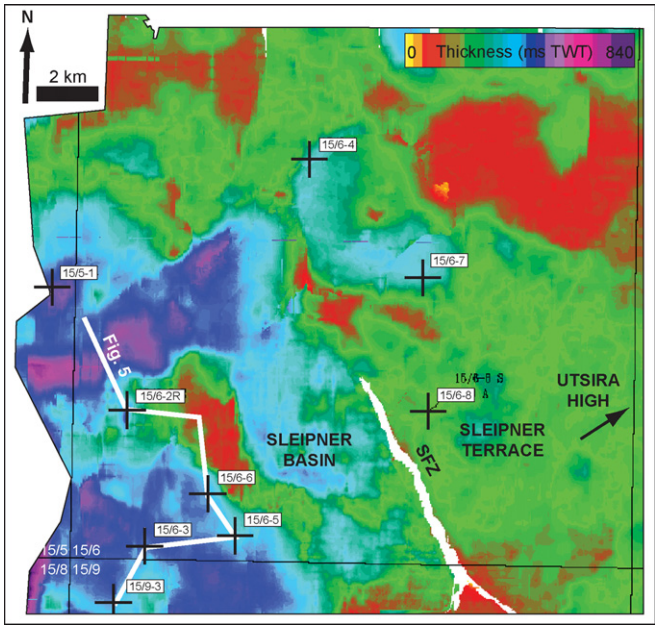

Fig. 6. Seismic isochron of the Triassic to Middle Jurassic succession (thickness in TWTT). Structural highs that flank the Sleipner Basin are characterised by amorphous Triassic and Middle Jurassic depocentres that formed within areas of salt withdrawal bound by salt-cored diapirs and pillows.

4.2. Triassic–early Middle Jurassic (pre-rift) mobility of the Zechstein Supergroup

The Triassic to early Middle Jurassic unit thickens westwards, from 20–50 ms (25–70 m) across parts of the Utsira High to 840 ms (1125 m) towards the axis of the South Viking Graben (Fig. 6). However, significant local variations in thickness are observed, particularly across the structural highs that bound the Sleipner Basin. For example, to the west of the basin, the unit reaches up to 600 ms (805 m) in thickness within a series of large (2–5 km wide) depocentres that are either completely isolated or connected by narrow (10–100's of metres width) 'corridors' (Figs. 5 and 6). These depocentres are flanked by salt-cored structural highs, over which the unit thins to 0–200 ms (0–268 m).

Whilst the overall WSW increase in the thickness of the Triassic to early Middle Jurassic succession reflects activity on the Graben Boundary Fault Zone in the far west (Thomas and Coward, 1996), the local thickness variations described above are attributed to mobility of the Zechstein Supergroup. The pattern of thickness distribution indicates that many of the large salt bodies adjacent to the Sleipner Basin formed through passive diapirism (e.g. Jackson et al., 1994; Davison et al., 2000; Rowan et al., 2003; Stewart, 2006; Hudec and Jackson, 2007) during the Triassic to early Middle Jurassic. The morphology and distribution of the salt bodies appears independent of the late Middle to Late Jurassic structural framework, i.e. they are largely amorphous and do not display the linearity that might be expected of fault-controlled structures. The passive diapirism was caused by differential loading of the evaporites by the Smith Bank, Skagerrak and Sleipner formations, which led to the development of salt withdrawal basins surrounded by rising salt walls (cf. Hodgson et al., 1992; Smith et al., 1993; Clark et al., 1998; Cartwright et al., 2001; Stewart, 2007). The role of passive diapirism in controlling Triassic to early Middle Jurassic sediment distribution has also been demonstrated across the Sleipner Terrace and SW flank of the Utsira High, located approximately 4 km east of the study area (Jackson et al., in press).

5. Structural style of the Sleipner Basin

The Sleipner Basin is approximately 30 km long by 8 km wide and is oriented broadly N–S; switching from a NE–SW orientation at the northern end, to a NNW–SSE orientation of the central and southern parts (Fig. 3). The NNW–SSE trending part of the basin is bound to the east by a normal fault, termed the Sleipner Fault Zone (SFZ), and to the west by a large salt-cored high (Figs. 3 and 7a and b). The SFZ has a maximum displacement of 900 ms (1200 m), although variable folding in its hangingwall results in displacement being locally as little as 200 ms (268 m). At top Bathonian level, the SFZ tips-out northwards, with the remainder of the eastern basin margin consisting of a broad monocline (Fig. 3).

Whilst the evolution of the SFZ forms the focus of this study, it is important to note that additional structures of NE–SW and NW–SE orientation significantly influence the geometry of the Sleipner Basin and the basin-bounding high to the east (Sleipner Terrace). Firstly, a broad monocline of NE–SW orientation is interpreted along the southeastern boundary of the northern part of the Sleipner Basin (Figs. 3 and 7c). Secondly, a series of NE-SW oriented faults are identified across the Sleipner Terrace, the largest (140 m throw) and most northerly of which dips to the northwest (Fig. 7c). To the south, a major NW-SE oriented, southwesterly dipping fault

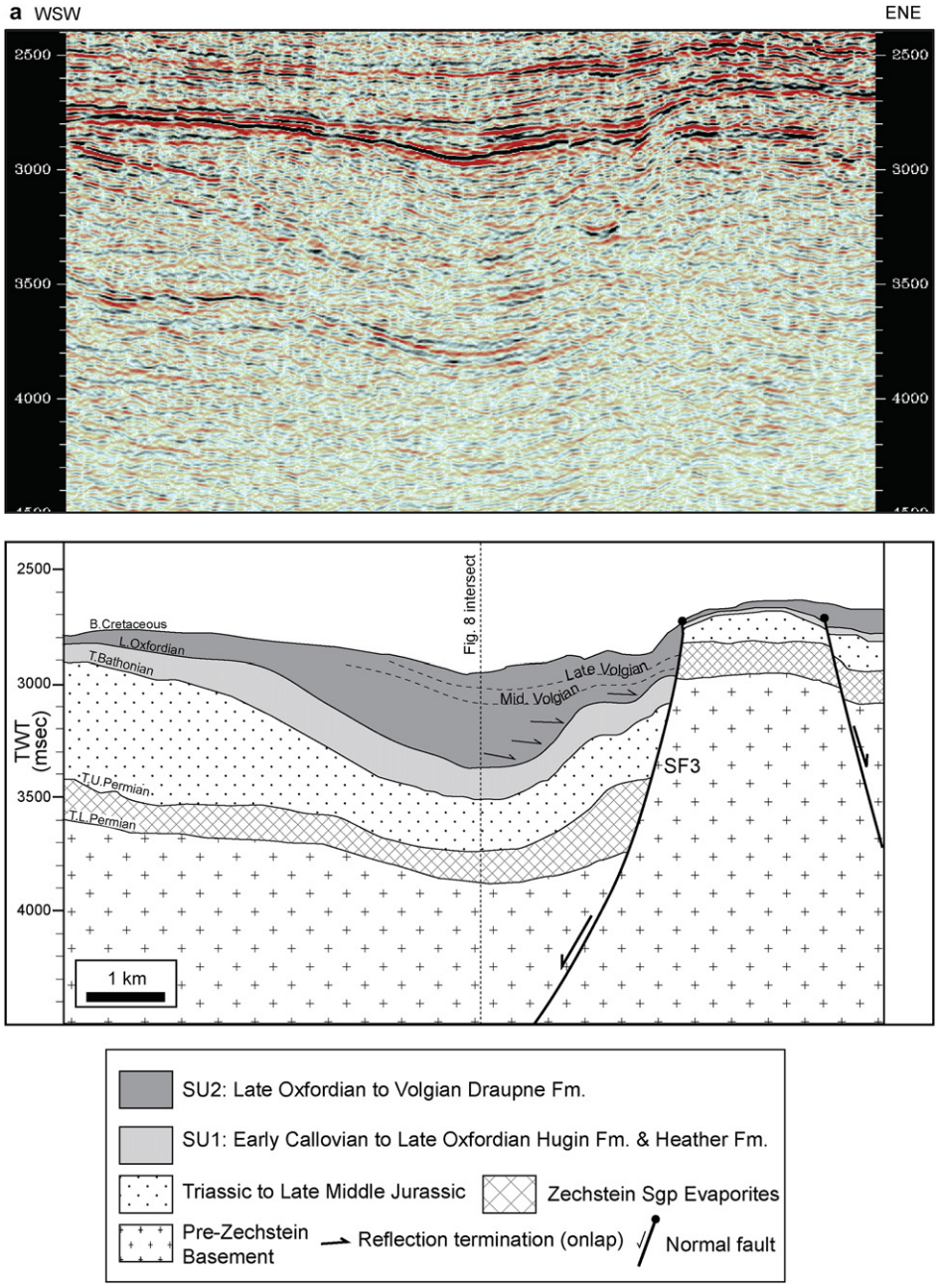

Fig. 7. Basin-transverse seismic profiles (a) Structural style of sub-basins associated with the SFZ (SB4). *Top Upper Permian*, *top Bathonian* and *Late Oxfordian* horizons dip away from the SFZ, forming a broad, monoclinal fold structure in the immediate hangingwall. Thickness of the salt increases towards the fault. (b) Structural style associated with intra-basin highs (IBHB). A broad fold structure is developed in the immediate hangingwall of the fault and the late syn-rift interval thins towards the fault. Increase in salt thickness towards the fault is much less pronounced than within sub-basins. (c) Structural style of sub-basin one (SB1). The southeastern basin margin is characterised by a broad monoclinal structure at *Top Bathonian* level, underlain by a normal fault at *Top Lower Permian* level. There is an increase in thickness of salt beneath the monoclinal structure. See text for full discussion.

(Volve Fault Zone) separates the Sleipner Terrace from the Volve Terrace (Fig. 3).

Two types of fold are observed in the Sleipner Basin in the hangingwall of the SFZ; (i) fault-perpendicular anticlines and synclines, and (ii) a fault-parallel monocline. The geometries of these two types of structure are described below.

5.1. Fault-perpendicular folds: Intra-basin highs and sub-basins

Three fault-perpendicular anticlines or intra-basin highs (IBHA-C) compartmentalise the Sleipner Basin along-strike into four synclinal sub-basins (SB1-4; Figs. 3 and 8). Two of these highs (IBHB & C) and three of the sub-basins (SB2-4) are located in the hangingwall of the SFZ. The intra-basin highs are underlain by salt pillows and have hinges which trend perpendicular (e.g. IBHB; Fig. 3) or sub-perpendicular (e.g. IBHC; Fig. 3) to local fault strike. At the structural level of the *top Bathonian* horizon, the highs have ~ 300 ms (400 m) amplitude and are 2.5–3 km wide, extending across the width of the Sleipner Basin.

Structural analysis indicates that the distribution of SB2-4 and salt-cored intra-basin highs B and C display a direct relationship to the structure of the SFZ (Fig. 3). Analysis of throw-length profiles for the *top Bathonian* (supra-salt) and *top Lower Permian* (sub-salt) seismic horizons reveals a series of throw minima which are

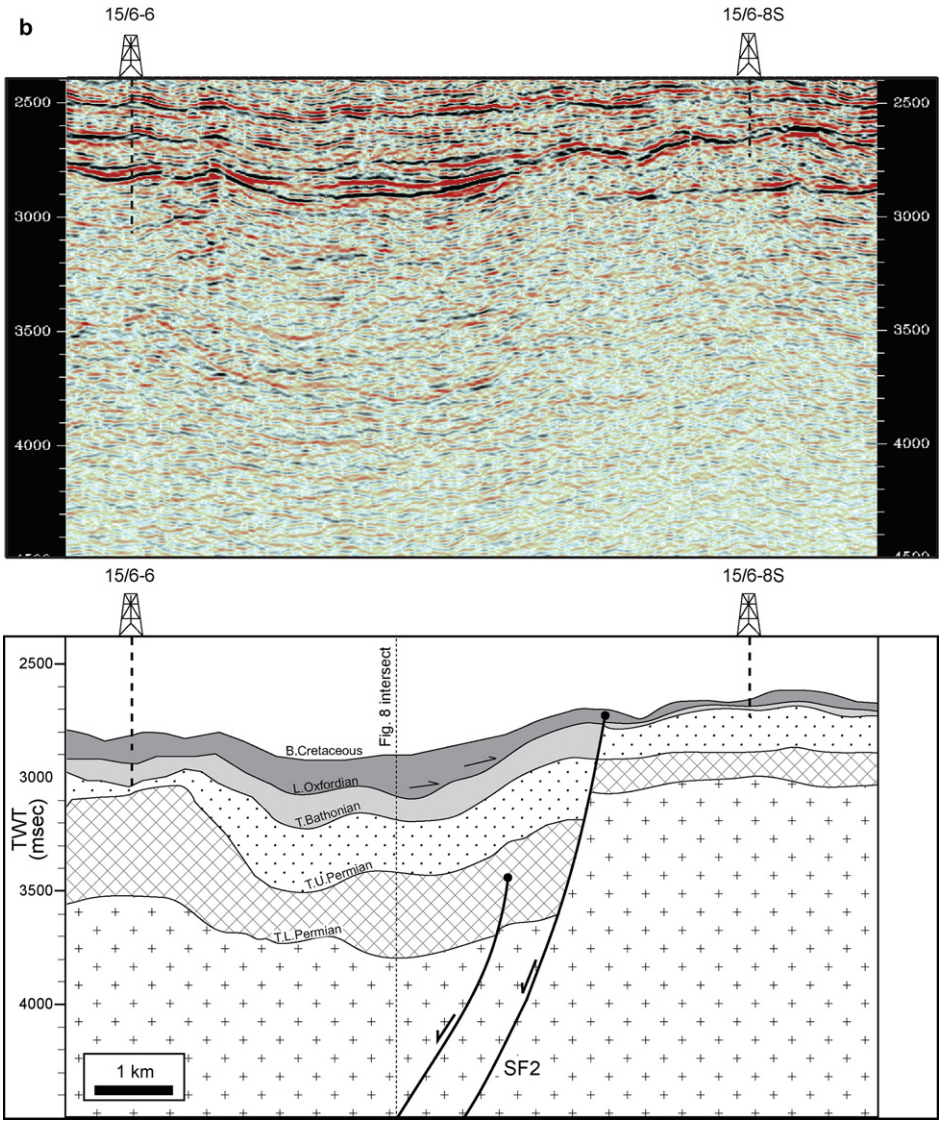

Fig. 7. (*continued*).

coincident with the fault-perpendicular, salt-cored intra-basin highs and throw maxima which are coincident with centres of sub-basins (Fig. 9). Along-strike variations in displacement commonly reflect the segmentation and linkage history of a normal fault (e.g. Peacock and Sanderson, 1991; Anders and Schlische, 1994; Cartwright et al., 1995) and it is thus suggested that the SFZ initially comprised three fault segments (SF1-3), one bounding each of sub-basins two, three and four (SB2-4). The pre-existing tips of these fault segments are identified by zones of displacement minima, located adjacent to the intra-basin highs. The *top Bathonian* profile demonstrates the lack of displacement across the SF1 segment as, at this stratigraphic level, this part of the basin margin is characterised by a broad monocline. The variation between throw maxima and minima at top Lower Permian level are smaller than observed for the *top Bathonian* horizon, the significance and origin of which is discussed further in later sections.

A series of intra-basin normal faults, oriented perpendicular to the basin strike, are identified in the northern part of the basin (Figs. 3 and 8). SB1, which is bound on its southeasterly margin by a broad monocline, is constrained at its north-eastern and south-western margins by NW-striking, south-westerly dipping listric faults which detach downwards onto the Zechstein Supergroup and result in the formation of a small graben immediately above the underlying salt-cored high (Fig. 8). These low-displacement faults are interpreted as relatively minor structures related to movement of the underlying salt. SB2 is kidney-shaped in map-view due to its location at an intersection between NE–SW and NW–SE trending structural grains. At the intersection point, a narrow (1 km wide) horst, bound to the north and south by ESE-striking normal faults, accommodates the transition from the NNW–SSE trend of the SFZ to the NE–SW trend of the blind monocline structure that bounds the southeastern side of SB1.

5.2. Fault-parallel fold

A NNW–SSE striking, fault-parallel fold is interpreted in the immediate hangingwall of the SFZ (Figs. 3 and 7a and b). This fold is up to 2 km wide, 368 ms (493 m) in amplitude and comprises a steep (~24°), west-dipping limb. Although well-developed in supra-Zechstein Supergroup units, the fold is absent within sub-salt units. Instead, the *top Lower Permian* seismic horizon has a horizontal to sub-horizontal cut-off with the SFZ (Fig. 7a and b) and, to accommodate the difference in folding between sub-salt and supra-salt units, the Zechstein Supergroup thickens eastwards

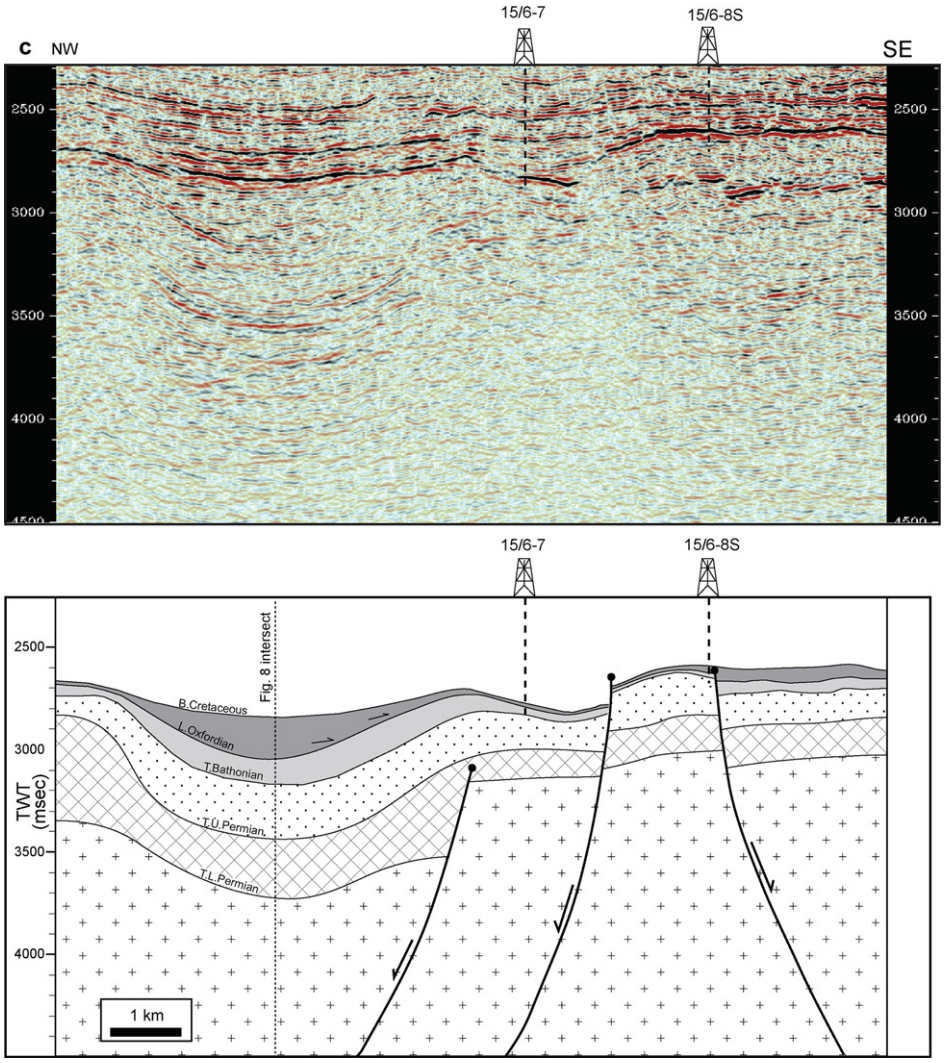

Fig. 7. (*continued*).

towards the SFZ. The magnitude of this eastwards thickening is variable along-strike, such that a greater increase towards the SFZ is observed at sub-basin locations than at intra-basin high locations (e.g. faultward increases of 200 ms (270 m) and 25 ms (35 m) beneath SB4 and IBHB, respectively; see Fig. 7a and b).

6. Seismic-stratigraphy of the Sleipner Basin

Having established the present-day geometry of late Middle to Late Jurassic rift-related structures, the seismic-stratigraphic architecture of the pre-rift (Triassic-early Middle Jurassic), and syn-rift (late Middle to Upper Jurassic) units must be analysed to constrain the spatial and temporal evolution.

6.1. Triassic–early Middle Jurassic (Pre-Rift)

Within the Sleipner Basin, the Triassic to Middle Jurassic succession is broadly isochronous (175–225 ms or 235–300 m), with only slight thickness variations identified in association with intra-basin highs (Figs. 6 and 8). Thus, although the salt-cored intra-basin highs may have had a subtle topographic expression during the Triassic to Middle Jurassic, it is suggested that their most pronounced period of growth occurred subsequent to the Bathonian during the late Middle to Late Jurassic rift episode.

6.2. Late Middle Jurassic–Upper Jurassic (syn-rift)

Because this study is focused on the inter-relationships between normal fault growth, salt mobility and syn-rift sedimentation, the detailed seismic stratigraphic analysis of the Upper Jurassic that follows is restricted to the part of the basin bounded by the SFZ. Here, fault growth history can be reconstructed and associated with distribution and thickness variations of salt and syn-rift depocentres. The origin and development of the NE–SW trending part of the basin (i.e. SB1) will be incorporated into the overall model of basin development in later sections.

Within the Sleipner Basin, the syn-rift unit reaches a maximum thickness of approximately 500 ms (670 m) and generally thins (to 150–250 ms or 200–335 m) across the intra-basin highs that separate the component sub-basins (Fig. 10). Locally thick areas are observed across the western flanks of the intra-basin highs, suggesting that the sub-basins were inter-connected for at least part of the rift phase. In addition to along-strike thickness variations, the syn-rift succession thins eastwards towards the SFZ (Fig. 10), from a maximum of 400–500 ms (540–670 m) in the centre of each sub-basin to 40–140 ms (55–190 m) in the immediate hangingwall of the fault. As such, the principal syn-rift depocentre is offset *ca.* 3 km into the axis of the basin.

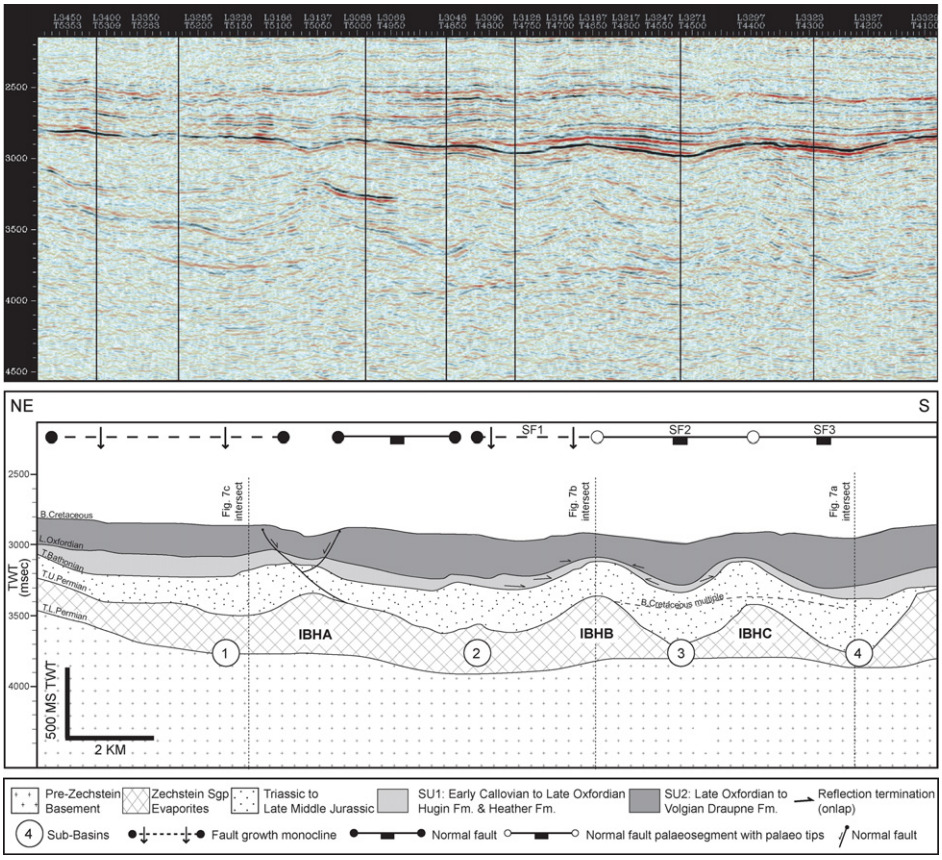

Fig. 8. Seismic profile demonstrating along-strike geometry of the Sleipner Basin. Early Callovian to early Volgian (late Middle to Late Jurassic) age salt-cored highs partition the basin into four sub-basins (SB1-4). Projected locations of palaeo-segments and palaeo-segment tips along the SFZ and the monoclinal structure that bounds SB1 are schematically shown.

Mapping of an intra-syn rift seismic horizon, tentatively dated as approximately 156 Ma (i.e. *Late Oxfordian* or near top Heather Formation), allowed subdivision of the interval into 'early' (SU1; Early Callovian-Late Oxfordian) and 'late' (SU2; Late Oxfordian–Volgian) units (Fig. 2). Although the syn-rift package as a whole thins towards the SFZ, SU1 displays only subtle thinning of the early syn-rift towards the fault (Figs. 7 and 11a). Along-strike, SU1 thins markedly across the intra-basin highs (Fig. 11a) and seismic cross-sections indicate that the lowermost reflections within this interval onlap the highs (Fig. 8). In contrast, thinning of SU2 towards the SFZ is significant and is associated with onlap of the lowermost reflections within the unit onto the base-bounding, *Late Oxfordian* reflection event (Figs. 7a and 11b). Along-strike, SU2 thins across the intra-basin highs and thickens into the adjacent sub-basins, although this variation is less pronounced than observed for SU1 (Figs. 8 and 11b).

Within SB4, two additional seismic reflection events were locally mapped (*Middle Volgian* and *Late Volgian*; Fig. 12), permitting the definition of three sub-units (SU2a-c) within SU2. SU2a, the lowermost stratal sub-unit, thickens westwards away from the SFZ and defines a depocentre offset *ca.* 4.5 km into the axis of the Sleipner Basin (Fig. 12a). In contrast, overlying stratal sub-units SU2b and SU2c thicken eastwards towards the SFZ, defining a depocentre that is focussed within the immediate hangingwall of the structure (Fig. 12b).

7. Development of late Middle to Late Jurassic (syn-rift) fold structures

The fault-perpendicular and fault-parallel fold structures within the Sleipner Basin are distinguished from latest Jurassic to early Cretaceous inversion-related folds identified elsewhere within the South Viking Graben (Thomas and Coward, 1996; Jackson and Larsen, 2008) in terms of both their age and their mechanism of development. Both fold types are interpreted as extensional in origin and developed during the late Middle to Late Jurassic rift event. The origin and timing of each are described separately here, before the relationships between the two types are considered.

7.1. Origin and timing of the fault-parallel monocline

Based on the interpreted late Middle to Late Jurassic age of the SFZ and the relationship between the cross-sectional geometry of the linked fault-fold and the thickness of the Zechstein Supergroup, the fault-parallel monocline is interpreted as a fault-propagation fold or forced fold (*sensu* Withjack et al., 1990). Along the length of the basin, the Zechstein salt thickens eastwards towards the SFZ beneath the steep limb of the monocline. The linearity of this thickened salt body differs significantly from the more amorphous, irregularly distributed salt structures observed elsewhere in the study area. Accordingly, this period of mobility can be linked to late Middle to Late Jurassic activity on the SFZ, rather than earlier passive diapirism during the Triassic to early Middle Jurassic.

It is interpreted that during early extension, the SFZ, which nucleated within the sub-salt 'basement', did not have sufficient displacement to hard-link through the evaporites of the Zechstein Supergroup (Fig. 13). The supra-salt cover strata were thus folded into a fault-parallel monocline, the axial trace of which was parallel to the underlying blind fault tip. Thickening of the Zechstein Supergroup towards the fault resulted from lateral flow of the

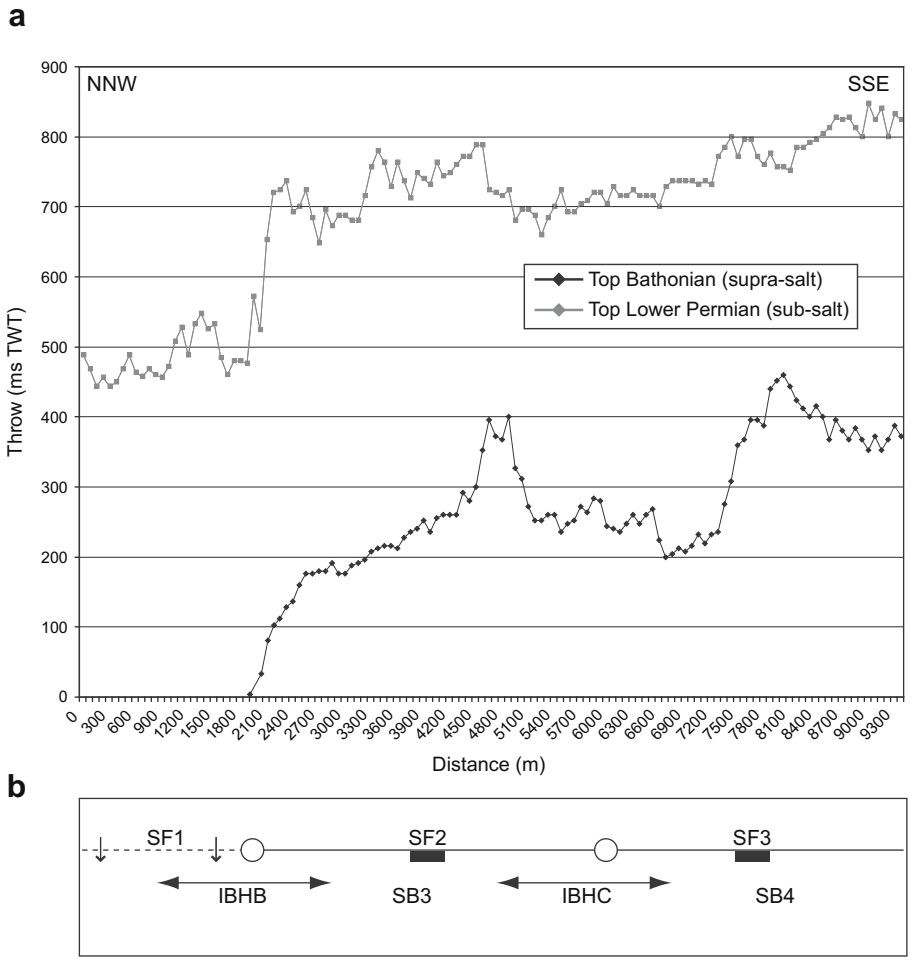

Fig. 9. (a) Fault throw profiles illustrating the along-strike variation in throw of *top Bathonian* and *top Lower Permian* horizons across the SFZ. (b) Position of pre-existing SFZ fault segments (SF1-3), intra-basin highs (IBHB&C), and sub-basins at *Top Bathonian* level. Areas of displacement maxima are located adjacent to fault segment centres (coinciding with sub-basins) whilst areas of displacement minima are located adjacent to zones of fault overlap (coinciding with intra-basin highs). See text for full discussion.

mobile evaporites into accommodation space in the immediate hangingwall of the SFZ (Fig. 13b).

The seismic–stratigraphic architecture of the pre-rift and syn-rift units provides temporal constraints on the evolution of the fault-propagation fold. Although a Permo-Triassic rift event is known to have affected the area regionally (e.g. Pegrum and Ljones, 1984; Ziegler, 1990; Glennie, 1990, 1995), seismic observations provide no clear evidence that the SFZ was an active structure at this time. Thickness of the pre-rift (Triassic to Late Middle Jurassic) interval remains relatively consistent towards the SFZ, indicating that upward propagation of the fault through the Zechstein Supergroup, and the consequent development of the fault-propagation fold, post-dated its deposition. If the SFZ were a pre-existing Permo-Triassic structure that was reactivated during the late Middle to Late Jurassic rift event, the effects of fault propagation on Zechstein evaporite mobility would be apparent within this supra-salt, pre-rift stratigraphic interval.

Thinning of SU1 towards the SFZ and the associated west-dipping limb of the hangingwall monocline, constrains the initiation of folding, and therefore the onset of sub-salt fault propagation, to the early stages (i.e. Early Callovian to Late Oxfordian) of the late Middle to Late Jurassic rift event (Figs. 7 and 11). As a result, the early syn-rift succession was deposited within a series of synclinal depocentres which were offset from the future position of the basin-bounding SFZ (Fig. 13b). Locally mapped intra-syn-rift units within SB4 document eastwards migration of this syn-rift depocentre from the basin axis to the immediate hangingwall of the fault (Fig. 12). During the early part of the late syn-rift, these depocentres remained offset from the future surface trace of the SFZ, as indicated by onlap of SU2a onto the top of the underlying, folded SU1 (Figs. 12a and 13c).

Breaching of the fault-propagation fold is interpreted to have occurred during the mid to late syn-rift (i.e. latest SU2a), resulting in displacement at the depositional surface (Figs. 12b and 13c). Lack of biostratigraphically constrained markers within the late Middle to Upper Jurassic syn-rift succession hinders accurate dating of this breaching but, as the main eastward shift of the depocentre is not observed until the upper part of the Draupne Formation (i.e. SU2b; Figs. 12b and 13c), a Volgian-age is proposed. However, as low rates of sedimentation associated with deposition of hemipelagic mudstones of the Draupne Formation could be outpaced by the rate of generation of fault and fold-related accommodation space, the basin may have been underfilled at the time of breaching. If this were the case, the time of breaching would pre-date the age of the first stratal units that are observed to thicken towards the fault (Fig. 13c).

Apparent thinning of the SU2b unit towards the northernmost part of SF3 could indicate that the fault-propagation fold was breached later in this area. Such diachronous breaching could reflect variable displacement rates along the SF3 palaeosegment. As palaeo-fault tips are associated with zones of lower displacement, it is proposed that the fault may have breached the upper surface of

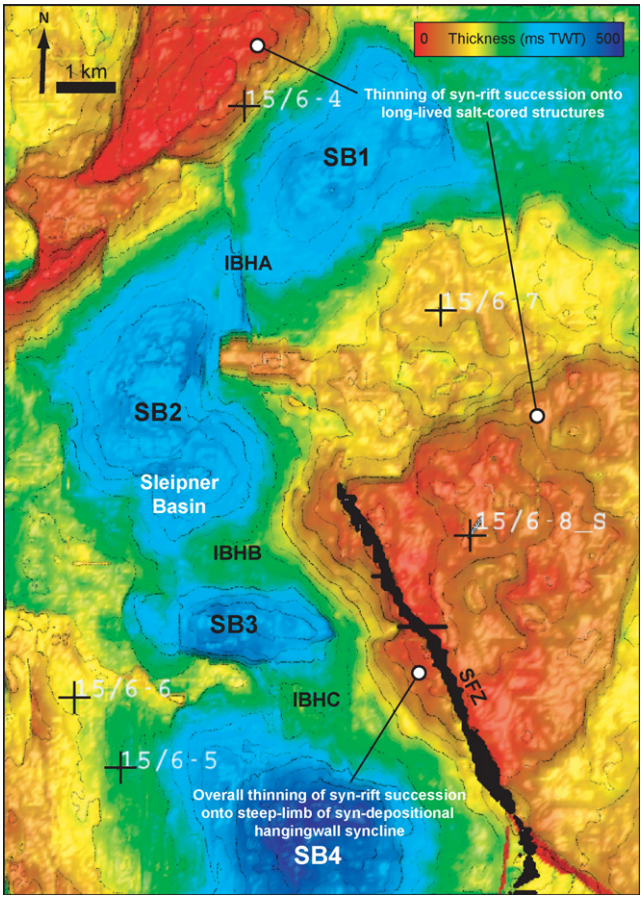

Fig. 10. Seismic isochron map of the entire latest Middle to Upper Jurassic syn-rift (*top Bathonian* to *BCU*) succession. See Fig. 3 for explanation of SB and IBH abbreviations. Overall, the main syn-rift depocentre is offset from the SFZ by the presence of the fault-parallel, hangingwall fold. Sediment also thins across the intra-basin, salt-cored highs.

the Zechstein Supergroup later in this tip location than at the higher displacement, segment centre.

Although not included in the detailed seismic stratigraphic analysis, interpretation of seismic cross-sections suggests that the NE-SW trending, northern part of the basin (SB1) was also influenced by the development of a fault-propagation fold (Figs. 3 and 7c). It is suggested that the southeastern margin of SB1 is bound by a monocline that, in contrast to the fold associated with the SFZ, remains unbreached, i.e. there is a NE-SW oriented normal fault at depth that failed to breach the top of the Zechstein salt layer. Ongoing development of this fold throughout the rift phase resulted in condensation of Upper Jurassic strata at the southeastern basin margin and offset of the sedimentary depocentre into the centre of the basin.

7.2. Origin and timing of fault-perpendicular folds

Although geometrically similar to some of the smaller Triassic to early Middle Jurassic-age salt-related structures observed in surrounding areas, Zechstein Supergroup salt pillows within the Sleipner Basin are deemed to be associated with the late Middle to Late Jurassic rift event and growth of the SFZ. This interpretation is based on the spatial relationship between the salt-cored intra-basin highs and throw variations along the basin-bounding SFZ, in combination with the seismic-stratigraphic architecture of pre- and syn-rift units.

As discussed previously, the positions of SB2-4, and their intervening intra-basin highs, show a clear relationship to the geometry of the SFZ (Figs. 3 and 9). Intra-basin highs are common in many rift basins, and the structures within the Sleipner Basin are interpreted as displacement-gradient folds (*sensu* Withjack et al., 2002) related to throw variations along the basin-bounding SFZ (cf. Schlische, 1995; McLeod et al., 2000). Intra-basin highs coincide with zones of throw minima, which are likely to represent pre-existing segment linkage points, whereas sub-basins occur adjacent to areas of displacement maxima, which are likely to represent pre-existing isolated fault segments (Figs. 3 and 9). In addition to the intra-basin highs and lows associated with the SFZ (SB2-4 & IBHB & C), the intra-basin high (IBHA) between SB1 and SB2 is also deemed to be associated with a displacement minima, which in this case is located at the intersection between the SFZ and the NE-SW trending blind fault (Figs. 3 and 8).

In rift basins which lack a ductile unit at depth, observed fault-perpendicular folds are usually; (i) significantly smaller in amplitude than those observed here; (ii) 'active' for a shorter period of the rift phase and have a greatly diminished structural expression during the later rift period after fault segment linkage; and (iii) do not persist across the entire width of the basin, but typically die-out <500 m into the hangingwall (e.g. Schlische, 1995; Dawers and Underhill, 2000; McLeod et al., 2000; Young et al., 2001; Jackson et al., 2002; Gawthorpe et al., 2003).

The greater size, areal extent and temporal persistence of intra-basin highs within the Sleipner Basin can be explained by the presence of thickened salt at the points of segment linkage or overlap. As a greater amount of accommodation was generated in the immediate hangingwall of individual fault segments during early extension, the lateral flow of salt towards the SFZ is expected to have been greater in these locations. Thus, thicker salt is likely to have remained at the intra-basin high locations. This is well illustrated by comparing along-strike throw variations for the *top Lower Permian* and *top Bathonian* seismic horizons (Fig. 9). As the *top Lower Permian* horizon marks the base of the Zechstein Supergroup, its geometry should be unaffected by salt movement, and along-strike variations should be solely associated with the growth and linkage of the fault. Variability in the along-strike profile at *top Bathonian* level is much more pronounced than at *top Lower Permian* level. For example, when measured from the centre of SF2 to the centre of IBHC, the displacement gradient is approximately 0.04 (40 m or 30 ms/km) for the sub-salt, *top Lower Permian* horizon and approximately 0.14 (135 m or 100 ms/km) for the supra-salt, *top Bathonian* horizon (Figs. 9a and 14biii). As observed for the fault-parallel hangingwall monocline, this difference in folding between the two structural levels is accounted for by thickened salt at intra-basin high locations. If salt were absent, a more subtle variation in throw would be expected at *top Bathonian* level between intra-basin highs and lows.

Syn-rift stratigraphic thickness variations and patterns of onlap constrain the timing of development of the fault-perpendicular fold structures as coeval with deposition of SU1 (Figs. 8, 11 and 12a). Thinning of the lower part of the late syn-rift unit (i.e. lower part of SU2) across the highs suggests that the structures continued to develop into the Late Oxfordian and possibly into the Kimmeridgian and Volgian (Figs. 8, 11b and 12b).

8. Tectono-stratigraphic evolution of the Sleipner Basin

The analyses and key interpretations described above are integrated here to produce a synoptic model for the tectono-stratigraphic evolution of the part of the Sleipner Basin associated with the SFZ (Fig. 14). During the early syn-rift, the SFZ consisted of a series of isolated fault segments (SF1-3, Fig. 14a) which were

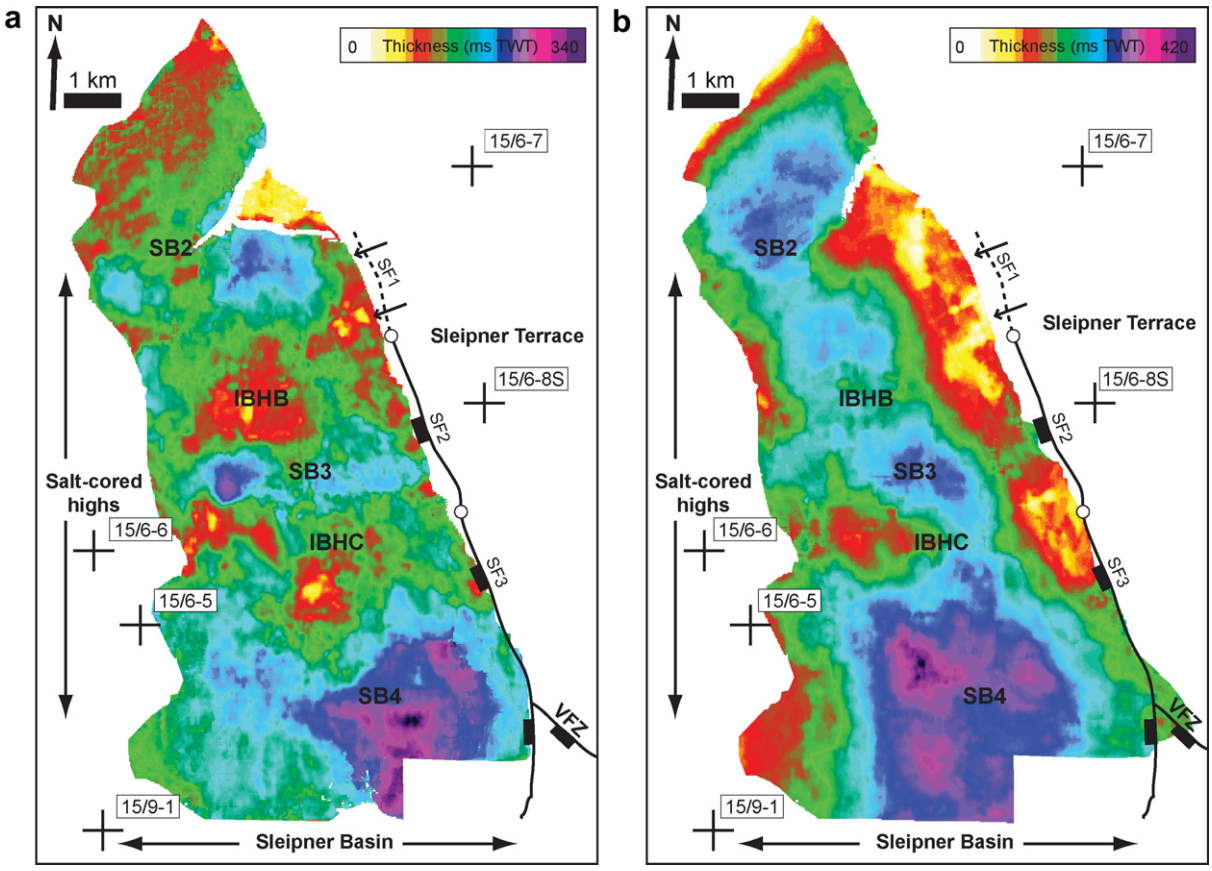

Fig. 11. Seismic isochrons of syn-rift units SU1 and SU2. See Fig. 3 for explanation of SB and IBH abbreviations and fault and fold symbology. (a) Thickness distribution of SU1 indicates that salt-cored intra-basin highs had a significant influence on early syn-rift sediment distribution. (b) Thickness distribution of SU2 illustrates the increasing influence of the fault-parallel fold on late syn-rift sedimentation. Depocentres are offset 2–3 km into the hangingwall of the SFZ; these are partially interconnected, suggesting less influence of the salt-cored intra-basin highs at this time.

restricted to the sub-salt basement. Each fault segment was overlain by a forced-fold, such that a series of en-echelon monoclines were present at the depositional surface. Sedimentation occurred 2–3 km basinward of these monoclines within sub-basins that were separated along-strike by fault-perpendicular intra-basin highs located at fault segment boundaries. The growth of the forced-folds within the supra-salt cover, combined with offset of the basement by the faults, led to the generation of accommodation that was filled by the eastwards migration of salt from beneath the sub-basins. At intra-basin highs, little movement of salt towards the SFZ occurred as these were associated with areas of little or no displacement or subsidence. It is suggested that sediment loading associated with relatively high depositional rates of the early syn-rift Hugin and Heather Formation sediments (Early Callovian to

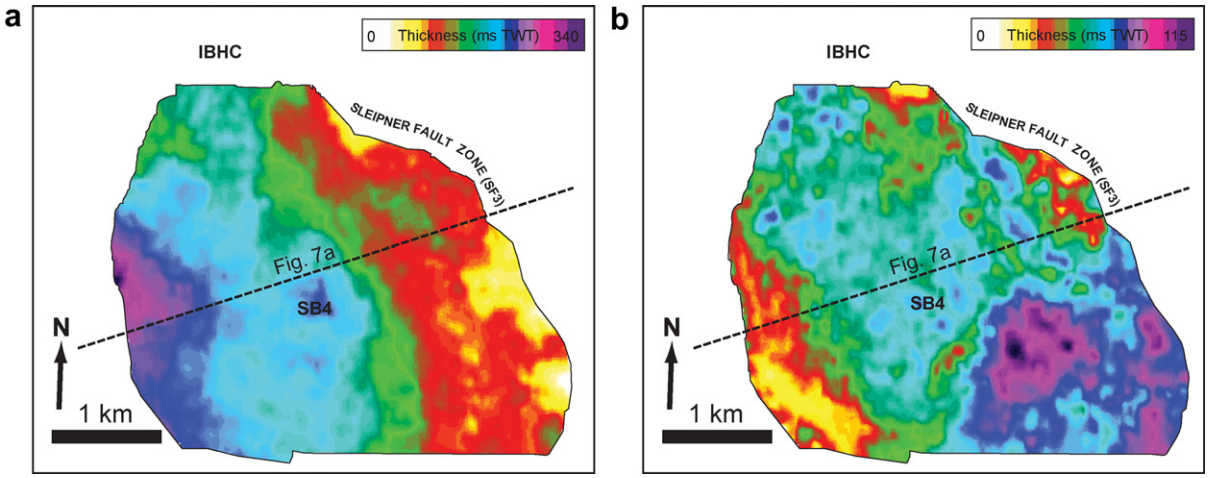

Fig. 12. Seismic isochrons of intra-SU2 units within Sub-Basin 4 (see Fig. 3 for regional context). (a) SU2a (Late Oxfordian to Middle Volgian) illustrates offset of main depocentre away from the SFZ towards the basin centre due to the growth of a forced fold at the basin margin at this time. (b) SU2b (Middle Volgian to Late Volgian) isochron illustrates shift of main depocentre towards SFZ due to breaching of the forced fold and accrual of fault displacement at the depositional surface.

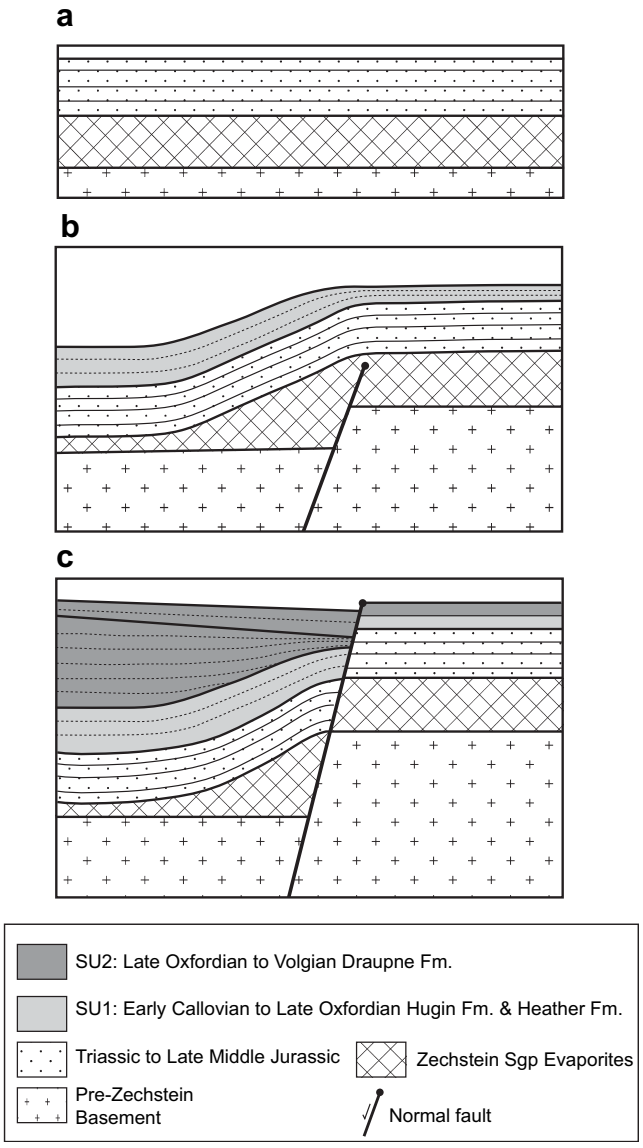

Fig. 13. Synoptic model illustrating the influence of extensional forced-fold development on syn-rift stratigraphic architecture (a) Geometry of basement, Zechstein Supergroup and pre-rift strata prior to fault propagation – units are assumed to be isochronous. (b) Early Callovian to Late Oxfordian (SU1). Upward fault propagation is inhibited by the presence of the salt, resulting in forced folding (*sensu* Withjack et al., 2002) of pre-rift cover strata and thinning of SU1 sediments towards the developing fold. (c) Late Oxfordian to Volgian (SU2). Early SU2 sediments onlap the upper surface of SU1 and continue to thin towards the fault until after the fault has breached the salt layer and overlying cover strata. This results in displacement at-surface and the migration of the depocentre towards the fault. Note that stage (c) is only applicable to the central and southern parts of the Sleipner Basin.

Late Oxfordian) may have been sufficient to trigger along-strike salt migration from beneath the sub-basins. This process of differential sediment loading and passive diapirism would further inflate the salt pillows that underpin the intra-basin highs (cf. Jackson et al., 1994; Davison et al., 2000; Rowan et al., 2003; Stewart, 2006; Hudec and Jackson, 2007).

The transition to the late syn-rift was characterised by: (i) vertical and lateral growth and linkage of the SFZ fault segments; (ii) ongoing forced folding; and (iii) an increase in the rate of salt migration from the basin centre towards the eastern basin margin along the entire length of the SFZ. The fault-parallel monocline had an increasing influence on overall basin geometry and the fault-perpendicular intra-basin highs began to subside as the segments of the SFZ became hard-linked. This segment linkage is likely to have been accompanied by increased rates of fault displacement which, in the case of the SF2 and SF3 parts of the fault, led to breaching of the forced fold and the subsequent generation of displacement at-surface (Fig. 14b). The northernmost part of the SFZ (SF1) failed to breach the salt layer and the fault-parallel monocline persisted in this area. Similarly, the NE-SW trending fault bounding the southeastern margin of SB1 remained blind throughout the rift phase. Any component of along-strike migration of salt due to differential loading is expected to have decreased during the late syn-rift as increased fault displacement rates on the now-linked SFZ are likely to have out-paced the low sedimentation rates associated with deposition of the latest Jurassic, Draupne Formation mudstones.

9. Discussion

9.1. Three-dimensional relationships between normal fault growth, fault-related folding and salt migration

Existing models describing the relationship between extensional faulting and salt migration within rift basins are largely two dimensional (e.g. Vendeville and Jackson, 1992a,b; Pascoe et al., 1999) and do not typically consider the early segmentation history of spatially related faults. We demonstrate here that three-dimensional seismic data can be used to reconstruct the growth history of large basin-bounding faults, and to investigate the temporal and spatial relationships between fault growth, fault-related fold development, and salt mobility (cf. Richardson et al., 2005). The presence of the salt-rich Zechstein Supergroup within the pre-rift succession led to enhanced fault-related folding during rifting, whilst the along-strike growth history of the fault zone appears to have had a significant impact on the temporal and spatial migration patterns of this ductile unit. One key observation is that patterns of salt migration were variable along-strike in direct association with the variable amounts and rates of displacement along the segmented fault system (Fig. 14).

The patterns of normal fault-related salt migration and distribution observed in this study can be compared and contrasted with those presented by Richardson et al. (2005) for the Revfallet Fault, Halten Terrace, offshore Mid-Norway. In their study, a single large salt swell, overlain by a forced fold, was identified in the immediate hangingwall of the central part of the fault. Isochron data demonstrates that the hangingwall of the Revfallet Fault is not compartmentalised into a series of sub-basins by salt-cored intra-basin highs. Thus, in the Sleipner Basin, the migration of salt during the syn-rift is deemed more spatially and temporally complex because the rate and amount of salt migration into the immediate hangingwall was variable along the length of the basin-bounding fault zone. In addition, there may have been a shift from predominantly axial (i.e. along fault strike) to predominantly lateral (i.e. dip-oriented) salt migration during fault growth due to changes in sedimentation rates and degrees of differential loading.

Differences in the style of fault-related evaporite mobility observed between this study and the Revfallet Fault example may be related to variability in the rate of development of the basin-bounding structures. In contrast to the SFZ, which evolved through the growth and linkage of initially isolated fault segments, the Revfallet Fault may have formed through the rapid lateral propagation of a single fault segment or through rapid linkage of individual segments in the early rift phase. This would have reduced the potential for differential rates of salt migration towards the fault and also decreased the likelihood of differential loading (and passive diapirism) of the evaporite-rich unit by syn-rift sediment.

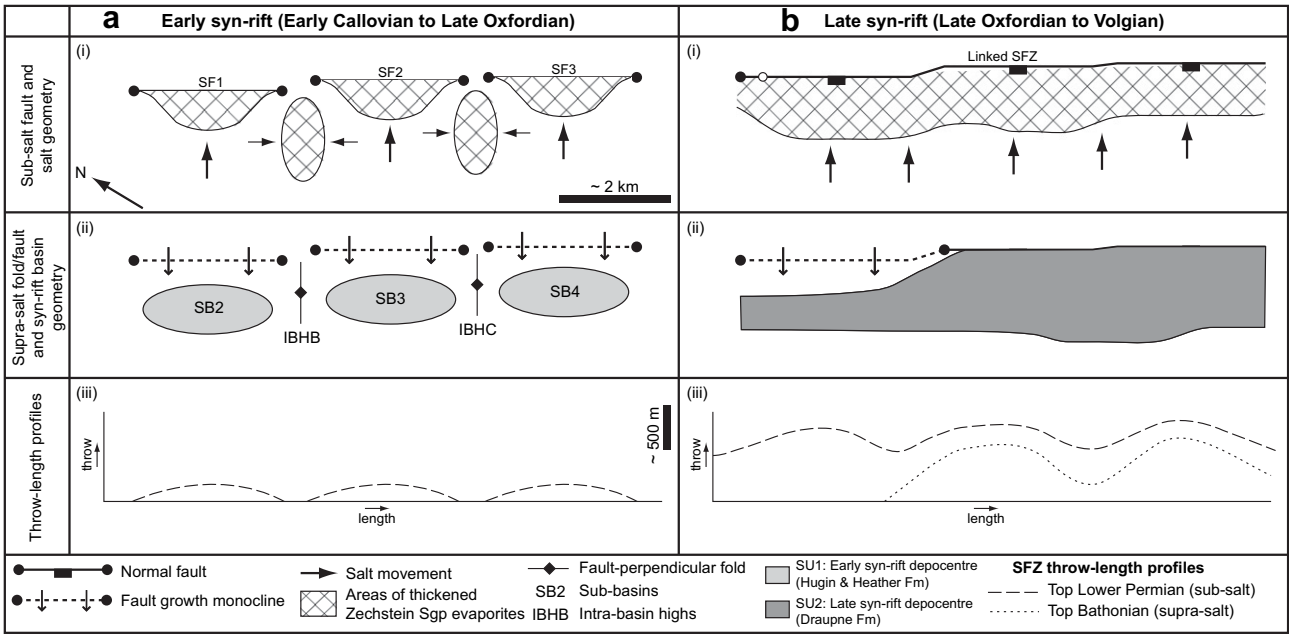

Fig. 14. Schematic model illustrating the relationships between extensional faulting, salt movement and sedimentary depocentre development in the part of the Sleipner Basin bounded by the SFZ. The model is divided into two time intervals; (a) early syn-rift (Early Callovian to Late Oxfordian) and (b) late syn-rift (Late Oxfordian to Volgian). Each time interval summarises (i) sub-salt fault geometry and patterns of salt migration, (ii) supra-salt fold/fault geometry and sedimentary depocentre development and (iii) displacement-length relationships for the SFZ based on data shown in Fig. 9. In the early syn-rift (a), a series of isolated fault segments displaced the base of salt and sub-salt strata whilst forced folds developed in the cover strata. Each forced fold was associated with a sedimentary depocentre, offset 2–3 km from the basin margin. Sediment loading within these depocentres may have contributed to the migration of salt towards the zones of displacement minima (i.e. intra-basin highs). In the late syn-rift (b), segment linkage and increased displacement across the SFZ, combined with lower sedimentation rates during Draupne Formation deposition, led to preferential migration of salt towards the fault. Reduced topographic expression of the intra-basin highs resulted in a more continuous late syn-rift depocentre. The central and southern parts of the SFZ (SF2 and 3) eventually breached the Zechstein Supergroup and overlying cover strata resulting in a shift of the depocentre towards the SFZ. Note that the depocentre associated with the northern part of the SFZ (i.e. SB2) remained offset because the fault failed to breach the salt in this part of the basin.

9.2. Syn-rift sedimentation in salt-influenced extensional basins

During the early stages of rifting, upward propagation of individual segments of the basin-bounding fault zone led to the formation of a series of at-surface, en-echelon monoclines which were flanked on their basinward side by isolated depocentres (Khalil and McClay, 2002). These early syn-rift depocentres were separated along-strike by intra-basin highs, located adjacent to fault segment boundaries. The presence of Zechstein salt within the pre-rift succession led to some notable differences in the patterns of syn-rift sedimentation typically observed in rift basins that lack a ductile unit. Most importantly, the development of the salt-related, monoclinal forced folds at the eastern basin margin resulted in the offset of the early syn-rift sedimentary depocentres a significant distance (2-3 km) into the hangingwall of the basin-bounding fault. Furthermore, due to the presence of large salt pillows beneath the structures, the intra-basin highs separating the depocentres were more pronounced and more temporally persistent than those documented in basins lacking salt layers within the basin-fill. Through time, the basin-bounding fault segments linked to become one through-going structure, causing the intra-basin highs to become increasingly less important in controlling the syn-rift stratal architecture. During the late syn-rift, breaching of the forced-fold by the through-going SFZ resulted in a more typical half-graben geometry, characterised by a faultward-diverging stratal wedge (Prosser, 1993; Gawthorpe et al., 1997).

10. Conclusions

1) The structural geometry of the Sleipner Basin was significantly influenced by the presence of a series of salt-related folds that interacted with, and were largely controlled by, the late Middle to Late Jurassic fault population. These comprise a fault-parallel fold structure in the immediate hangingwall of the Sleipner Fault Zone and a series of fault-perpendicular salt-cored anticlines that subdivide the basin along-strike.
2) The fault-parallel fold is interpreted as a fault-propagation fold, developed as a consequence of upward propagation of the Sleipner Fault Zone within strata containing the evaporite-rich, Zechstein Supergroup. Strata above this mechanically weak unit were folded ahead of the fault tip whilst strata beneath were subject to brittle faulting. Fault displacement analysis and patterns of syn-rift sediment distribution reveal that the Sleipner Fault Zone was initially segmented and that individual fault-propagation fold structures were associated with each of the segments. Upon segment linkage, and prior to surface breaching, the fault-propagation fold became continuous along the entire length of the SFZ.
3) The fault-perpendicular, salt-cored anticlines are interpreted as displacement gradient folds that developed adjacent to palaeo-tips of the SFZ. Fault displacement analysis clearly demonstrates that these salt-cored highs are associated with areas of displacement minima. The presence of thickened salt at points of pre-existing segment linkage resulted in displacement gradient folds that are larger in amplitude and longer-lived than similar structures observed in salt-absent rift basins. The amplification of the fold structures by salt is demonstrated by the comparison of lateral displacement gradients measured for sub-salt and supra-salt horizons.
4) This study demonstrates that the segmentation and linkage history of extensional faults can significantly impact the three-dimensional migration patterns of salt. Movement of salt during the late Middle to Late Jurassic was intimately

associated with the growth history of the Sleipner Fault Zone. Migration towards the fault zone was greatest in areas adjacent to fault segment centres, whilst thick pillows of salt remained in areas adjacent to fault segment tips. As rifting progressed, hard-linkage of the SFZ, and breaching of the fault-propagation fold, caused this along-strike variability to diminish.

5) The salt-related folds and evolving normal fault segments had a fundamental control on the size and distribution of sedimentary depocentres during the latest Middle and Late Jurassic. Early syn-rift depocentres (early Callovian to late Kimmeridgian/early Volgian) were offset into the centre of the basin by the development of the fault-parallel, fault-propagation fold and were also partitioned along-strike by the intra-basin, salt-cored, displacement gradient folds. In the later syn-rift (Volgian), once the Sleipner Fault Zone had hard-linked and subsequently breached the fault-propagation fold structure, the principal depocentre began to shift toward the immediate hangingwall and also became more continuous along-strike due to the reduced expression of the displacement gradient folds.
6) Whilst fault displacement along the SFZ is considered to be the primary control on Late Jurassic salt migration in the Sleipner Basin, it is suggested that sediment loading may have driven a component of this migration, particularly during the early stages of rifting. Salt-cored intra-basin highs could be amplified by axial movement of salt in response to deposition of early syn-rift shallow-marine sandstones and shelfal mudstones within sub-basins. The effects of sediment loading would be expected to dissipate as rifting progressed from the initiation to climax phase because fault displacement rates would begin to far-outpace sedimentation rates associated with deposition of deep-water mudstones.

Acknowledgments

We would like to thank Rachel Kieft, Gary Hampson, Martha Withjack, Anna-Sofia Gregersen, Unni Stalsberg Sjursen, Signe Ottesen and Tom Dreyer for contributing to discussions during the course of this study. Mary Ford, Jonathan Imber and one anonymous reviewer are thanked for constructive and thorough reviews which improved the manuscript. Thank you to Statoil for providing funding and to Landmark Graphics for access to OpenWorks software through provision of an Academic Licence Agreement to Imperial College. The views expressed in this paper are the authors and do not necessarily represent those of Statoil ASA or partners within the PL303 licence.

References

Anders, M.H., Schlische, R.W., 1994. Overlapping faults, intrabasin highs, and the growth of normal faults. Journal of the Geological Society 102, 165–179.

Badley, M.E., Price, J.D., Rambech Dahl, C., Agdestein, T., 1988. The structural evolution of the Northern Viking Graben and its bearing upon extensional modes of basin formation. Journal of the Geological Society 145, 455–472.

Bartholomew, I.D., Peters, J.M., Powell, C.M., 1993. Regional structural evolution of the North Sea: oblique-slip and reactivation of basement lineaments. In: Parker, J.R. (Ed.), Petroleum Geology of Northwest Europe: Proceedings of the 4th Conference. Geological Society, London, pp. 1109–1122.

Branther, S.R.F., 2003. The East Brae Field, Blocks 16/03a, 16/03b, UK North Sea. In: Gluyas, J.G., Hichens, H.M. (Eds.), United Kingdom Oil and Gas Fields, Commemorative Millennium Volume. Geological Society, London, Memoir, vol. 20, pp. 191–197.

Brehm, J., 2003. The North Brae and Beinn Fields, Blocks 16/7a, UK North Sea. In: Gluyas, J.G., Hichens, H.M. (Eds.), United Kingdom Oil and Gas Fields, Commemorative Millennium Volume. Geological Society, London, Memoir, vol. 20, pp. 199–209.

Brown, A.R., 2003. Interpretation of Three-Dimensional Seismic Data. American Association of Petroleum Geologists, Memoir 42, Society of Economic Geologists, Investigations, No. p. 6th edn.

Cartwright, J., Trudgill, B.D., Mansfield, C.S., 1995. Fault Growth and segment linkage: an explanation for scatter in maximum displacement and trace length data from the Canyonlands Grabens of Se Utah. Journal of Structural Geology 17, 1319–1326.

Cartwright, J.A., Stewart, S., Clark, J., 2001. Salt dissolution and salt-related deformation of the Forth Approaches Basin, UK North Sea. Marine and Petroleum Geology 18, 757–778.

Cherry, S.T.J., 1993. The interaction of structure and sedimentary process controlling deposition of the Upper Jurassic Brae Formation Conglomerate, Block 16/17, North Sea. In: Parker, J.R. (Ed.), Petroleum Geology of Northwest Europe: Proceedings of the 4th Conference, pp. 387–400.

Clark, J.A., Stewart, S.A., Cartwright, J.A., 1998. Evolution of the NW margin of the North Permian Basin, UK North Sea. Journal of the Geological Society of London 155, 663–676.

Corfield, S., Sharp, I.R., 2000. Structural style and Stratigraphic architecture of fault propagation folding in extensional settings: a seismic example from the Smørbukk area, Halten Terrace, Mid-Norway. Basin Research 12, 329–341.

Cockings, J.H., Gifford Kessler II, L., Mazza, T.A., Riley, L.A., 1992. Bathonian to mid-Oxfordian sequence stratigraphy of the South Viking Graben, North Sea. In: Hardman, R.F.P. (Ed.), Exploration Britain: Insights for the Next Decade. Geological Society, London, Special Publications, vol. 67, pp. 65–105.

Coward, M.P., 1995. Structural and tectonic setting of the Permo-Triassic basins of northwest Europe. In: Boldy, S.A.R. (Ed.), Permian and Triassic Rifting in Northwest Europe. Geological Society, London, Special Publication, vol. 91, pp. 7–39.

Dawers, N.H., Anders, M.H., 1995. Displacement–length scaling and fault linkage. Journal of Structural Geology 17, 607–614.

Dawers, N.H., Underhill, J.R., 2000. The role of fault interaction and linkage in controlling synrift stratigraphic sequences: Late Jurassic, Statfjord East Area, Northern North Sea. AAPG Bulletin 84, 45–64.

Davison, I., Alsop, I., Birch, P., Elders, C., Evans, N., Nicholson, H., Rorison, P., Wade, D., Woodward, J., Young, M., 2000. Geometry and late-stage structural evolution of Central Graben salt diapirs, North Sea. Marine and Petroleum Geology 17, 499–522.

Fisher, M.J., Mudge, D.C., 1998. Triassic. In: Glennie, K.W. (Ed.), Petroleum Geology of the North Sea: Basic concepts and recent advances. Blackwell, Oxford, pp. 212–244.

Fletcher, K.J., 2003a. The South Brae Field, Blocks 16/07a, 16/07b, UK North Sea. In: Gluyas, J.G., Hichens, H.M. (Eds.), United Kingdom Oil and Gas Fields, Commemorative Millennium Volume. Geological Society, London, Memoir, vol. 20, pp. 211–221.

Fletcher, K.J., 2003b. The Central Brae Field, Blocks 16/07a, 16/07b, UK North Sea. In: Gluyas, J.G., Hichens, H.M. (Eds.), United Kingdom Oil and Gas Fields, Commemorative Millennium Volume. Geological Society, London, Memoir, vol. 20, pp. 183–190.

Ford, M., Le Carlier de Veslud, C., Bourgeois, O., 2007. Kinematic and geometric analysis of fault-related folds in a rift setting: the Dannemarie basin, Upper Rhine Graben, France. Journal of Structural Geology 29, 1811–1830.

Fraser, S.I., Robinson, A.M., Johnson, H.D., Underhill, J.R., Kadolsky, D.G.A., Connell, R., Johannessen, P., Ravnas, R., 2003. Upper Jurassic. In: Evans, D., Graham, C., Armour, A., Bathurst, P. (Eds.), The Millennium Atlas: Petroleum Geology of the Central and Northern North Sea. The Geological Society, London, pp. 157–189.

Frostick, L.E., Linsey, T.K., Reid, I., 1992. Tectonic and climatic control on Triassic sedimentation in the Beryl Basin, northern North Sea. Journal of the Geological Society of London 149, 13–26.

Gawthorpe, R.L., Hurst, J.M., 1993. Transfer zones in extensional basins: their structural style and influence on drainage development and stratigraphy. Journal of the Geological Society 150, 1137–1152.

Gawthorpe, R.L., Fraser, A.J., Collier, R., 1994. Sequence stratigraphy in active extensional basins: implications for the interpretation of ancient basin fills. Marine and Petroleum Geology 11, 642–658.

Gawthorpe, R.L., Sharp, I., Underhill, J.R., Gupta, S., 1997. Linked sequence Stratigraphic and structural evolution of propagating normal faults. Geology 25, 795–798.

Gawthorpe, R.L., Jackson, C.A.L., Young, M.J., Sharp, I.R., Moustafa, A.R., Leppard, C. W., 2003. Normal fault growth, displacement localisation and the evolution of normal fault populations: the Hammam Faraun fault block, Suez rift, Egypt. Journal of Structural Geology 25, 883–895.

Glennie, K.W., 1990. Outline of North Sea history and structural framework. In: Glennie, K.W. (Ed.), Introduction to the Petroleum Geology of the North Sea. Blackwell, Oxford, pp. 34–77.

Glennie, K.W., 1995. Permian and Triassic rifting in Northwest Europe. In: Boldy, S.A. R. (Ed.), Permian and Triassic Rifting in Northwest Europe. Geol. Soc. of London, Spec. Publ., vol. 91, pp. 1–5.

Gupta, S., Cowie, P., Dawers, N.H., Underhill, J.R., 1998. A Mechanism to explain rift basin subsidence and stratigraphic patterns through fault array evolution. Geology 26, 595–598.

Gupta, S., Underhill, J.R., Sharp, I.R., Gawthorpe, R.L., 1999. Role of fault interactions in controlling synrift sediment dispersal patterns: Miocene, Abu Alaqa Group, Suez Rift, Sinai, Egypt. Basin Research 11, 167–189.

Harris, J.P., Fowler, R.M., 1987. Enhanced prospectivity of the Mid-Late Jurassic sediments of the South Viking Graben, northern North Sea. In: Brooks, J., Glennie, K. (Eds.), Petroleum Geology of Northwest Europe: Proceedings of the 4th Conference. Graham & Trotman, London, pp. 879–898.

Helland-Hansen, W., Ashton, M., Lømo, L., Steel, R.J., 1992. Advance and retreat of the Brent delta: recent contributions to the depositional model. In: Morton, A.C., Haszeldine, R.S., Giles, M.R., Brown, S. (Eds.), Geology of the Brent Group, vol. 61, pp. 109–128.

Hodgson, N.A., Farnsworth, J., Fraser, A.J., 1992. Salt-related tectonics, sedimentation and hydrocarbon plays in the Central Graben, North Sea, UKCS. In: Hardman, R. F.P. (Ed.), Exploration Britain: Insights for the Next Decade. Geological Society, London, Special Publication, vol. 67, pp. 31–63.

Hudec, M.R., Jackson, M.P.A., 2007. Terra infirma: understanding salt tectonics. Earth-Science Reviews 82, 1–28.

Husmo, T., Hamar, G., Høiland, O., Johannessen, E.P., Rømuld, A., Spencer, A., Titterton, R., 2003. Middle Jurassic. In: Evans, D., Graham, C., Armour, A., Bathurst, P. (Eds.), The Millennium Atlas: Petroleum Geology of the Central and Northern North Sea. The Geological Society, London, pp. 128–155.

Jackson, M.P.A., Vendeville, B.C., 1994. Regional extension as a geologic trigger for diapirism. Geological Society of American Bulletin 106, 57–73.

Jackson, M.P.A., Vendeville, B.C., Ela-Schultz, D.D., 1994. Structural dynamics of salt systems. Annual Review of Earth and Planetary Sciences 22, 93–117.

Jackson, C.A.L., Gawthorpe, R.L., Sharp, I.R., 2002. Growth and linkage of the East Tanka fault zone, Suez rift: structural style and syn-rift stratigraphic response. Journal of the Geological Society of London 159, 175–187.

Jackson, C.A.-L., Larsen, E., 2008. Temporal constraints on basin inversion provided by 3D seismic and well data: a case study from the South Viking Graben. Basin Research 20, 397–417.

Jackson, C.A.L., Kane, K.E., Larsen, E. Structural evolution on the Utsira High; implications for Jurassic sediment dispersal and reservoir distribution. Petroleum Geoscience, in press.

Khalil, S.M., McClay, K.R., 2002. Extensional fault-related folding, northwestern Red Sea, Egypt. Journal of Structural Geology 24, 743–762.

Koyi, H., Jenyon, M.K., Petersen, K., 1993. The effect of basement faulting on diapirism. Journal of Petroleum Geology 16, 285–312.

Knott, S.D., 2001. Gravity-driven crustal shortening in failed rifts. Journal of the Geological Society 158, 193–196.

Knott, S.D., Burchell, M.T., Jolley, E.T., Fraser, A.J., 1993. Mesozoic to Cenozoic plate reconstructions of the North Atlantic margins. In: Parker, J.R. (Ed.), Petroleum Geology of Northwest Europe: Proceedings of the 4th Conference. Geological Society, London, pp. 953–974.

Knott, S.D., Beach, A., Welbon, A.I., Brockbank, P.J., 1995. Basin inversion in the Gulf of Suez. In: Buchanan, J.G., Buchanan, P.G. (Eds.), Basin Inversion, vol. 88, pp. 59–82.

Marsh, N., Imber, J., Holdsworth, R.E., Brockbank, P., Ringrose, P., 2009. The structural evolution of the Halten Terrace, offshore Mid-Norway: extensional fault growth and strain localisation in a multi-layer brittle-ductile system. Basin Research. doi:10.1111/j.1365-2117.2009.00404.x.

McLeod, A.E., Dawers, N.H., Underhill, J.R., 2000. The propagation and linkage of normal faults: insights from the Strathspey–Brent–Statfjord fault array, northern North Sea. Basin Research 12, 263–284.

McLeod, A.E., Underhill, J.R., Davies, S.J., Dawers, N.H., 2002. The influence of fault array evolution syn-rift sedimentation patterns: Controls on deposition in the Strathspey–Brent–Statfjord half-graben, northern North Sea. AAPG Bulletin 86, 1061–1093.

Mitchener, B.C., Lawrence, D.A., Partington, M.A., Bowman, M.B.J., Gluyas, J., 1992. Brent group: sequence stratigraphy and regional implications. In: Morton, A.C., Haszeldine, R.S., Giles, M.R., Brown, S. (Eds.), Geology of the Brent Group. Geological Society, London, vol. 61, pp. 45–80.

Pascoe, R., Hooper, H., Storhaug, K., Harper, H., 1999. Evolution of extensional styles at the southern termination of the Nordland Ridge, mid-Norway: a response to variations in coupling above Triassic salt. In: Fleet, A.J., Boldy, S.A.R. (Eds.), Petroleum Geology of Northwest Europe: Proceedings of the 5th Conference, pp. 83–90.

Peacock, D.C.P., Sanderson, D.J., 1991. Displacements, segment linkage and relay ramps in Normal Fault Zones. Journal of Structural Geology 13, 721–733.

Pegrum, R.M., Ljones, T.E., 1984. 15/9 Gamma gas field offshore Norway, new trap type for North Sea Basin with regional structural implications. American Association of Petroleum Geologists Bulletin 68, 874–902.

Penge, J., Munns, J.W., Taylor, B., Windle, T.M.F., 1999. Rift-raft tectonics: examples of gravitational tectonics from the Zechstein basins of Northwest Europe. In: Fleet, A.J., Boldy, S.A.R. (Eds.), Petroleum Geology of Northwest Europe: Proceedings of the 5th Conference. Geol Soc, London, pp. 201–213.

Prosser, 1993. Rift-related linked depositional systems and their seismic expression. In: Williams, G.D., Dobb, A. (Eds.), Tectonics and Seismic Sequence Stratigraphy. Geol. Soc. Spec. Publ., vol. 71, pp. 35–66.

Riba, O., 1976. Syntectonic unconformities of the Alto Cardener, Spanish Pyrenees: a genetic interpretation. Sedimentary Geology 15, 213–233.

Richardson, N.J., Underhill, J.R., Lewis, G., 2005. The Role of evaporite mobility in modifying subsidence patterns during normal fault growth and linkage, Halten Terrace, Mid-Norway. Basin Research 17, 203–223.

Roberts, A.M., Yielding, G., Kusznir, N.J., Walker, S.J., 1995. Quantitative analysis of Triassic extension in the North Viking Graben. Journal of the Geological Society 152, 15–26.

Rowan, M.G., Lawton, T.F., Giles, K.A., Ratliff, R.A., 2003. Near-salt deformation in La Popa basin, Mexico, and the northern Gulf of Mexico: a general model for passive diapirism. American Association of Petroleum Geologists Bulletin 87, 733–756.

Schlische, R.W., 1995. Geometry and origin of fault-related folds in extensional settings. AAPG Bulletin 79, 1611–1678.

Sharp, I.R., Gawthorpe, R.L., Armstrong, B., Underhill, J.R., 2000. Propagation history and passive rotation of mesoscale normal faults: implications for synrift stratigraphic development. Basin Research 12, 285–305.

Smith, R.I., Hodgson, N., Fulton, M., 1993. Salt control on Triassic reservoir distribution. In: Parker, J.R. (Ed.), Petroleum Geology of Northwest Europe: Proceedings of the 4th Conference. Geological Society of London, pp. 547–557.

Stewart, S.A., Harvey, M.J., Otto, S.C., Weston, P.J., 1996. Influence of salt on fault geometry: examples from the UK salt basins. In: Alsop, G.I., Blundell, D.J., Davison, I. (Eds.), Salt Tectonics. Geol. Soc. of London Spec. Publ., vol. 100, pp. 175–202.

Stewart, S.A., Ruffell, A.H., Harvey, M.J., 1997. Relationship between basement-linked and gravity-driven fault systems in the UKCS salt basins. Marine and Petroleum Geology 14, 581–604.

Stewart, S.A., Clark, J.A., 1999. Impact of salt on the structure of the Central North Sea hydrocarbon fairways. In: Fleet, A.J., Boldy, S.A.R. (Eds.), Petroleum Geology of Northwest Europe: Proceedings of the 5th Conference. Geological Society of London, pp. 179–200.

Stewart, S.A., 2006. Implications of passive salt diapir kinematics for reservoir segmentation by radial and concentric faults. Marine and Petroleum Geology 23, 843–853.

Stewart, S.A., 2007. Salt tectonics in the North Sea Basin: a structural style template for seismic interpreters. In: Ries, A.C., Butler, R.W.H., Graham, R.H. (Eds.), Deformation of the Continental Crust: The Legacy of Mike Coward. Geological Society, London, Special Publications, vol. 272, pp. 361–396.

Thomas, D.W., Coward, M.P., 1995. Late Jurassic-early Cretaceous inversion of the Northern East Shetland Basin, Northern North Sea. In: Buchanan, J.G., Buchanan, P.G. (Eds.), Basin Inversion, vol. 88, pp. 275–306.

Thomas, D.W., Coward, M.P., 1996. Mesozoic regional tectonics and South Viking Graben formation: evidence for localized thin-skinned detachments during rift development and inversion. Marine and Petroleum Geology 13, 149–177.

Underhill, J.R., Partington, M.A., 1993. Jurassic thermal doming and deflation in the North Sea: implications of the sequence stratigraphic evidence. In: Parker, J.R. (Ed.), Petroleum Geology of Northwest Europe: Proceedings of the 4th Conference. Geological Society of London, pp. 337–345.

Vendeville, B.C., Jackson, M.P.A., 1992a. The rise of diapirs during thin-skinned extension. Marine and Petroleum Geology 9, 331–353.

Vendeville, B.C., Jackson, M.P.A., 1992b. The fall of diapirs during thin-skinned extension. Marine and Petroleum Geology 9, 354–371.

Vendeville, B., Hongxing, G., Jackson, M.P.A., 1995. Scale models of salt tectonics during basement-involved extension. Petroleum Geoscience 1, 177–183.

Withjack, M.O., Olson, J., Petersen, E., 1990. Experimental models of extensional forced folds. AAPG Bulletin 74, 1038–1054.

Withjack, M.O., Callaway, S., 2000. Active normal faulting beneath a salt layer: an experimental study of deformation patterns in the cover sequence. AAPG Bulletin 84, 627–651.

Young, M.J., Gawthorpe, R.L., Hardy, S., 2001. Growth and linkage of a segmented normal fault zone; the Late Jurassic Murchison-Statfjord North Fault, northern North Sea. Journal of Structural Geology 23, 1933–1952.

Young, M.J., Gawthorpe, R.L., Sharp, I.R., 2002. Architecture and evolution of syn-rift clastic depositional systems towards the tip of a major fault segment. Basin Research 14, 1–23.

Ziegler, P.A., 1990. Tectonic and palaeogeographic development of the North Sea rift system. In: Blundell, D.J., Gibbs, A.D. (Eds.), Tectonic Evolution of the North Sea Rifts. International Lithosphere Programme, vol. 81, pp. 1–36.